

Elucidating the Chemical Dynamics of the Elementary Reactions of the 1-Propynyl Radical ($\text{CH}_3\text{CC}\cdot$; X^2A_1) with Methylacetylene (H_3CCCH ; X^1A_1) and Allene (H_2CCCH_2 ; X^1A_1)

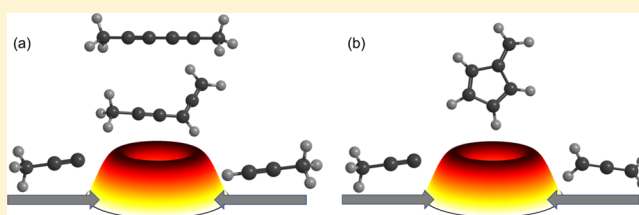
Chao He,[†] Long Zhao,[†] Aaron M. Thomas,[†] Alexander N. Morozov,[‡] Alexander M. Mebel,^{*,‡} and Ralf I. Kaiser^{*,†}

[†]Department of Chemistry, University of Hawai'i at Manoa, Honolulu, Hawaii 96822, United States

[‡]Department of Chemistry and Biochemistry, Florida International University, Miami, Florida 33199, United States

Supporting Information

ABSTRACT: The reactions of the 1-propynyl radical ($\text{CH}_3\text{CC}\cdot$; X^2A_1) with two C_3H_4 isomers, methylacetylene (H_3CCCH ; X^1A_1) and allene (H_2CCCH_2 ; X^1A_1), along with their (partially) deuterated counterparts were explored at collision energies of 37 kJ mol^{-1} , exploiting crossed molecular beams to unravel the chemical reaction dynamics to synthesize distinct C_6H_6 isomers under single collision conditions. The forward convolution fitting of the laboratory data along with ab initio and statistical calculations revealed that both reactions have no entrance barrier, proceed via indirect (complex-forming) reaction dynamics involving C_6H_7 intermediates with life times longer than their rotation period(s), and are initiated by the addition of the 1-propynyl radical with its radical center to the π -electron density of the unsaturated hydrocarbon at the terminal carbon atoms of methylacetylene (C1) and allene (C1/C3). In the methylacetylene system, the initial collision complexes undergo unimolecular decomposition via tight exit transition states by atomic hydrogen loss, forming dimethyldiacetylene ($\text{CH}_3\text{CCCCCH}_3$) and 1-propynylallene ($\text{H}_3\text{CCCHCCCH}_2$) in overall exoergic reactions (123 and 98 kJ mol^{-1}) with a branching ratio of 9.4 ± 0.1 ; the methyl group of the 1-propynyl reactant acts solely as a spectator. On the other hand, in the allene system, our experimental data exhibit the formation of the fulvene ($c\text{-C}_5\text{H}_4\text{CH}_2$) isomer via a six-step reaction sequence with two higher energy isomers—hexa-1,2-dien-4-yne ($\text{H}_2\text{CCCHCCCH}_3$) and hexa-1,4-diyne ($\text{HCCCH}_2\text{-CCCH}_3$)—also predicted to be formed based on our statistical calculations. The pathway to fulvene advocates that, in the allene–1-propynyl system, the methyl group of the 1-propynyl reactant is actively engaged in the reaction mechanism to form fulvene. Because both reactions are barrierless and exoergic and all transition states are located below the energy of the separated reactants, the hydrogen-deficient C_6H_6 isomers identified in our investigation are predicted to be synthesized in low-temperature environments, such as in hydrocarbon-rich atmospheres of planets and their moons such as Titan along with cold molecular clouds such as Taurus Molecular Cloud-1.



1. INTRODUCTION

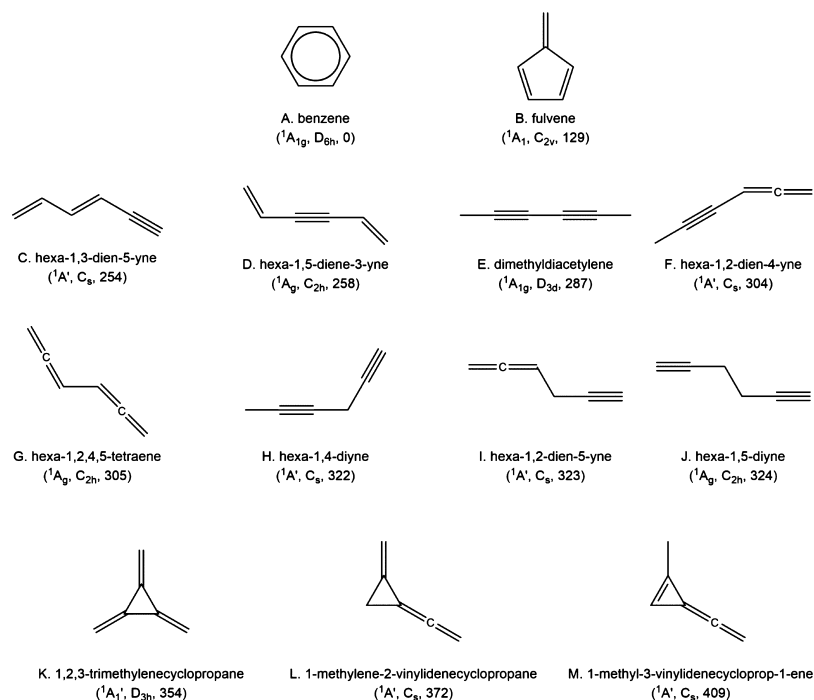
During the last decade, the untangling of the reaction dynamics and energetics leading to the formation of distinct C_6H_6 isomers has received considerable attention from the reaction dynamics,¹ combustion,^{2–7} and astrochemistry communities.⁸ Classified as the most fundamental building block of polycyclic aromatic hydrocarbons (PAHs)^{2,3,9–21}—organic molecules composed of fused benzene rings—benzene (C_6H_6 , D_{6h}) represents not only the simplest neutral 6π Hückel aromatic hydrocarbon molecule but also the thermodynamically most stable structure among all 216 C_6H_6 isomers (Scheme 1).^{15,22} Dinadayalane et al. computed the C_6H_6 potential energy surface (PES), exploiting ab initio [Møller–Plesset perturbation theory and coupled cluster single and double substitution method with a perturbative treatment of triple excitation (CCSD(T))] and hybrid density functional theory (B3LYP) calculations with the triple- ζ basis set.¹⁵ Mebel, Lin, and co-workers calculated the isomerization pathways between the

most favorable C_6H_6 isomers and their decomposition channels using the chemically accurate G2M model chemistry approach.^{23–27} Scheme 1 depicts selected C_6H_6 isomers in the order of increasing relative energies with respect to benzene (0 kJ mol^{-1}). These isomers can be sorted into three classes: (1) monocyclic isomers with a six-membered (A) and five-membered ring (B); (2) acyclic molecules (C to J), and (3) cyclic molecules with a three-membered ring (K to M). Among these isomers, fulvene (B) was first prepared by Thiele in 1900²⁸ and represents a prototype of a class of exotic hydrocarbons formally obtained by cross-conjugating one ring and a methylenic moiety through an exocyclic carbon–carbon double bond. Several acyclic C_6H_6 isomers such as hexa-1,3-dien-5-yne (C), hexa-1,2,4,5-tetraene (G), hexa-1,2-dien-5-yne (I), and

Received: April 22, 2019

Revised: June 5, 2019

Published: June 9, 2019

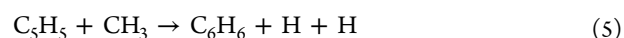
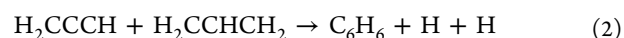
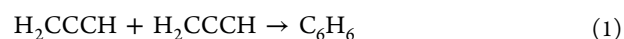
Scheme 1. Structures of Selected C₆H₆ Isomers^a

^aPoint groups and energies (kJ mol⁻¹) relative to benzene are also shown. Energies were obtained from ref 15.

hexa-1,5-diyne (J) were observed in the reaction of self-recombination of the propargyl radical (C₃H₃)^{29,30} and in the pyrolysis of hexa-1,5-diyne (J).³¹ Isomers carrying a three-membered ring such as 1,2,3-trimethylenecyclopropane (K), 1-methylene-2-vinylidenecyclopropane (L), and 1-methyl-3-vinylidenecycloprop-1-ene (M) are among the thermodynamically least stable C₆H₆ structures and hold strong tendencies to either decyclize or dimerize.¹⁵ Hence, these isomers have not yet been observed in combustion flames or in the interstellar medium (ISM).³²

The thermodynamically most stable isomer—benzene—has been observed in combustion flames,^{2–7} in the ISM,⁸ and in our solar system.^{33,34} The majority of the experimental and theoretical investigations indicate that benzene (C₆H₆) and the phenyl radical (C₆H₅) might be formed involving reactions of resonantly stabilized free radicals including propargyl (H₂CCCH) self-combination (1),^{10,35} the reaction of propargyl (H₂CCCH) with allyl (H₂CCHCH₂) (2),⁴ the reaction of acetylene (C₂H₂) with the *n*- and/or *i*-1,3-butadien-1-yl radical (C₄H₅)⁵ (3), collisions of acetylene (C₂H₂) with the *n*-1-buten-3-yn-1-yl radical (C₄H₃)^{6,36} followed by third body stabilization (4),^{5,6} and the radical–radical recombination of methyl (CH₃) with cyclopentadienyl (C₅H₅) (5).^{14,37} Under single collision conditions as provided in crossed molecular beam experiments, benzene and phenyl are synthesized via the barrierless, bimolecular gas-phase reactions of 1,3-butadiene (C₄H₆) with ethynyl (C₂H)¹ and dicarbon (C₂),³⁸ respectively (6 and 7). Fulvene, a higher energy isomer of benzene, has been suggested to play a critical role in the formation of benzene.^{4,7,10,39–41} Hansen et al. pointed out that benzene might be formed via fulvene in allene (CH₂CCH₂) and methylacetylene (CH₃CCH) flames involving reactions of propargyl (C₃H₃) with C₃H₄ molecules (8).^{40–42} Fulvene is predicted to be the major product in the reactions of C₃H₃ + C₃H₃ (1), C₃H₃ + C₃H₅ (2), and C₃H₅ + CH₃ (5) under combustion conditions.^{4,10,35,36,39} The key pathways to

benzene are suggested to involve hydrogen atom-assisted isomerization of fulvene.^{4,10,18,39–41}



The aforementioned compilation reveals that the untangling of the formation mechanisms of fulvene along with its isomers under single collision conditions is still in its infancy. Here, we access the C₆H₆ and C₆H₇ PESs via the barrierless reactions of the 1-propynyl radical (CH₃CC) with methylacetylene (CH₃CCH) and allene (CH₂CCH₂). By combining the experimental results, including selective isotopic labeling with electronic structure calculations, we provide compelling evidence that several high-energy C₆H₆ isomers—among them fulvene—can be formed via barrierless elementary reactions under single collision conditions *excluding* hydrogen-assisted isomerization processes, thus providing an unprecedented approach of elucidating the primary reaction products formed.

2. EXPERIMENTAL AND COMPUTATIONAL METHODS

2.1. Experimental Methods. The reactions of 1-propynyl (CH₃CC; X²A₁) with methylacetylene (CH₃CCH; X¹A₁), methylacetylene-*d*₄ (CD₃CCD; X¹A₁), methyl-*d*₃-acetylene

(CD₃CCH; X¹A₁), methylacetylene-*d*₁ (CH₃CCD; X¹A₁), allene (CH₂CCH₂; X¹A₁), and allene-*d*₄ (CD₂CCD₂; X¹A₁) were studied under single collision conditions, exploiting a universal crossed molecular beams machine at the University of Hawaii.⁴³ In the primary source chamber, the pulsed 1-propynyl molecular beam was produced by photodissociation of 1-bromopropyne (CH₃CCBr; 1717 ChemMall, 95%) seeded at a level of 0.5% in helium (99.9999%; AirGas) at 193 nm (Complex 110, Coherent, Inc.) at 60 Hz and 20 mJ per pulse. This gas mixture—stored in a Teflon-lined sample cylinder⁴⁴—was regulated to 760 Torr and introduced into a piezoelectric pulsed valve operating at 60 Hz at pulse widths of 80 μs and peak voltages of −400 V. The pulsed 1-propynyl beam passes through a skimmer and is velocity-selected by a four-slot chopper wheel rotating at 120 Hz. On-axis (Θ = 0°) characterization of the primary beam determines a peak velocity v_p of 1759 m s^{−1} and a speed ratio *S* of 8.3 (Table 1).

Table 1. Peak Velocities (v_p) and Speed Ratios (*S*) of 1-Propynyl (CH₃CC), Methylacetylene (CH₃CCH), Methylacetylene-*d*₄ (CD₃CCD), Methyl-*d*₃-acetylene (CD₃CCH), Methylacetylene-*d*₁ (CH₃CCD), Allene (CH₂CCH₂), and Allene-*d*₄ (CD₂CCD₂) Beams along with the Corresponding Collision Energies (E_C) and CM Angles (Θ_{CM}) for Each Reactive Scattering Experiment

beam	v_p (m s ^{−1})	<i>S</i>	E_C (kJ mol ^{−1})	Θ _{CM} (deg)
C ₃ H ₃ (X ² A ₁)	1767 ± 10	8.0 ± 0.3		
CH ₃ CCH (X ¹ A ₁)	800 ± 10	12.0 ± 0.4	37.1 ± 0.4	25.7 ± 0.3
CD ₃ CCD (X ¹ A ₁)	790 ± 10	12.0 ± 0.4	38.7 ± 0.4	27.5 ± 0.3
CD ₃ CCH (X ¹ A ₁)	790 ± 10	12.0 ± 0.4	38.3 ± 0.4	27.0 ± 0.3
CH ₃ CCD (X ¹ A ₁)	800 ± 10	12.0 ± 0.4	37.6 ± 0.4	26.2 ± 0.3
C ₃ H ₃ (X ² A ₁)	1750 ± 8	8.6 ± 0.4		
CH ₂ CCH ₂ (X ¹ A ₁)	800 ± 10	12.0 ± 0.4	36.4 ± 0.3	25.9 ± 0.3
CD ₂ CCD ₂ (X ¹ A ₁)	790 ± 10	12.0 ± 0.4	37.3 ± 0.3	27.3 ± 0.3

The primary beam crosses perpendicularly the secondary supersonic beam of the hydrocarbon reactant generated in the secondary source chamber. In each reaction system, the hydrocarbon backing pressure was regulated to 550 Torr and fed into the secondary pulsed valve operated at a repetition rate of 60 Hz, a pulse width of 80 μs, and a peak voltage of −400 V. The methylacetylene and allene velocity distributions were determined to be $v_p = 800 ± 10$ m s^{−1} with *S* = 12.0 ± 0.4 resulting in nominal collision energies E_C of 37.1 ± 0.4 and 36.4 ± 0.3 kJ mol^{−1} and center-of-mass (CM) angles Θ_{CM} of 25.7 ± 0.3° and 25.9 ± 0.3°, respectively. The peak velocities and speed ratios along with the collision energies and CM angles for methylacetylene, methylacetylene-*d*₄, methylacetylene-*d*₃, methylacetylene-*d*₁, allene, and allene-*d*₄ are summarized in Table 1.

The machine operates a triply differentially pumped detector rotatable in the plane defined by both sources; this detector comprises a Brink-type ionizer,⁴⁵ a quadrupole mass spectrometer (QMS), and a Daly-type ion counter.⁴⁶ The neutral products formed in the reactive scattering process enter the detector and are ionized through electron impact at an electron energy of 40 eV, at a current of 1.4 mA, and an ion flight

constant of 4.25 μs amu^{−1/2} and then filtered according to mass-to-charge (*m/z*) ratios using the QMS (Extrel; QC 150) equipped with a 2.1 MHz oscillator. The ions are then accelerated by a negative 22.5 kV potential onto an aluminum-coated stainless steel target, thus generating a cascade of secondary electrons that is directed toward an aluminum-coated scintillator. The resulting signal is collected by a photomultiplier tube (Burle, model 8850) operated at a negative potential of 1.35 kV. The signal output is discriminated at 1.6 mV (Advanced Research Instruments, model F-100TD) and recorded by a multichannel scaler (SRS 430).

Time-of-flight (TOF) spectra were recorded at laboratory (LAB) angles in the range of 0° ≤ Θ ≤ 69° with respect to the 1-propynyl radical beam (Θ = 0°). The TOF spectra were then integrated and normalized to obtain the product angular distribution in the LAB frame. To obtain information on the reaction dynamics, a forward convolution method is used to transform the LAB data into the CM frame.^{47–50} This represents an iterative method, whereby the user-defined CM translational energy $P(E_T)$ and angular $T(\theta)$ flux distributions are varied until a suitable fit of the LAB frame TOF spectra and angular distributions are achieved. The CM functions comprise the reactive differential cross-section $I(\theta, u)$, which is taken to be separable into its CM scattering angle θ and CM velocity u components, $I(u, \theta) \approx P(u) \times T(\theta)$. The differential cross-section is plotted as a flux contour map that serves as an image of the reaction. Errors of the $P(E_T)$ and $T(\theta)$ functions are determined within the 1σ error limits of the accompanying LAB angular distribution while maintaining a good fit of the LAB TOF spectra.

2.2. Computational Methods. Geometry optimization for the reactants, intermediates, transition states, and products on the C₆H₇ PES pertinent to the reactions of 1-propynyl radical with allene and methylacetylene were carried out on the density functional B3LYP level of theory^{51,52} with the 6-311G(d,p) basis set. Vibrational frequencies were computed on the same B3LYP/6-311G(d,p) level and were used for the evaluation of zero-point vibrational energy (ZPE) corrections and in calculations of rate constants. Single-point energies for all stationary structures were refined by single-point calculations using the explicitly correlated coupled clusters CCSD(T)-F12 method^{53,54} with Dunning's correlation-consistent cc-pVTZ-f12 basis set.⁵⁵ The expected accuracy of the CCSD(T)-F12/cc-pVTZ-f12//B3LYP/6-311G(d,p) + ZPE-(B3LYP/6-311G(d,p)) relative energies is within 4 kJ mol^{−1} or better.⁵⁶ The B3LYP and CCSD(T)-F12 calculations were performed using the GAUSSIAN 09⁵⁷ and MOLPRO 2010⁵⁸ program packages, respectively. Energy-dependent rate constants of all unimolecular reaction steps on the C₆H₇ PES following initial association of the 1-propynyl radical with the C₃H₄ isomers were computed using the Rice–Ramsperger–Kassel–Marcus (RRKM) theory.^{59–61} The available internal energy was taken as a sum of the collision energy and the chemical activation energy, that is, negative of the relative energy of a species with respect to the reactants. One energy level was considered throughout as a zero-pressure limit corresponding to crossed molecular beam conditions. The numbers and densities of states were computed within the harmonic approximation using the B3LYP/6-311G(d,p) frequencies. Product branching ratios were evaluated by solving first-order kinetic equations within steady-state approximation utilizing the RRKM rate constants for individual reaction steps. Rate constants for barrierless hydrogen atom

eliminations in the unimolecular decomposition of fulvene were computed using variational transitional-state theory.⁶² The RRKM and branching ratio calculations were carried out using a newly developed in-house code, which processes an output of GAUSSIAN 09 frequency calculations to carry out the direct count of the number of states for transition states and the density of states for local minima.

3. RESULTS

3.1. LAB Frame. For both the reactions of the 1-propynyl radical (CH_3CC ; 39 amu) with methylacetylene (CH_3CCH ; 40 amu) and allene (CH_2CCH_2 ; 40 amu), the reactive scattering signal was observed at mass-to-charge ratios (m/z) of 79 ($^{13}\text{C}_6\text{H}_6^+$), 78 (C_6H_6^+), and 77 (C_6H_5^+) formally connected to the adduct, the hydrogen loss reaction product, and the molecular hydrogen loss product, respectively. The TOF spectra recorded at these mass-to-charge ratios exhibited identical patterns after scaling with the signal at $m/z = 79$ collected at a level of about 7% of $m/z = 78$. These findings suggest that the signals at $m/z = 78$ and 77 originate from the same reaction channel forming the heavy product (C_6H_6 ; 78 amu) along with atomic hydrogen (H ; 1 amu); the signal at $m/z = 77$ can be attributed to dissociative electron impact ionization of the C_6H_6 product in the electron impact ionizer, whereas the ion counts at $m/z = 79$ can be correlated with the ^{13}C -substituted C_6H_6 product arising from the natural distribution of carbon atom isotopes. Therefore, having evidenced the hydrogen atom loss channel, the TOF spectra of the nascent C_6H_6 reaction product were collected at the best signal-to-noise ratio at $m/z = 78$ at distinct LAB angles from 15.25° to 45.25° in 2.5° intervals with up to 1.3×10^6 TOFs per angle (Figure 1); note that the signal at $m/z = 77$ was detected at a level of typically 128% compared to $m/z = 78$. Contributions from the nonreactive scattering of the primary beam, verified by scattering with argon, were subsequently subtracted from the TOF spectra close to the primary beam. The resulting TOFs were then normalized with respect to the CM angle (Θ_{CM}) to obtain the LAB angular distribution (LAD; Figure 2). Considering the interference from the primary beam, the lowest angle of the LAD can just reach 15.25° . The LAD distributions for both systems span nearly 30° within the scattering plane and are symmetric around Θ_{CM} . This result suggests indirect scattering dynamics and bound C_6H_7 reaction intermediate(s) dissociating to C_6H_6 plus atomic hydrogen.

In order to elucidate the detailed position(s) of the atomic hydrogen loss(es), the reactions of 1-propynyl radical (CH_3CC ; 39 amu) with (partially) deuterated methylacetylene and allene were performed as well. Isotopic substitution experiments present an ideal tool to extract the hydrogen atom loss position(s).^{63–69} First, these studies focused on the atomic hydrogen and deuterium loss channels of the 1-propynyl radical (CH_3CC ; 39 amu) with methylacetylene- d_4 (CD_3CCD ; X^1A_1 ; 44 amu), methyl- d_3 -acetylene (CD_3CCH ; X^1A_1 ; 43 amu), and methylacetylene- d_1 (CH_3CCD ; X^1A_1 ; 41 amu). For the 1-propynyl radical (CH_3CC ; 39 amu)–methylacetylene- d_4 (CD_3CCD) system (reactions 9 and 10), TOFs recorded at $m/z = 82$ ($\text{C}_6\text{H}_2\text{D}_4^+$) (9) and $m/z = 81$ ($\text{C}_6\text{H}_3\text{D}_3^+$) (10) at the CM angle of 26.8° suggest no signal at $m/z = 82$ (Figure 3a); ion counts were only observed at $m/z = 81$. Consequently, the signal at $m/z = 81$ is attributed to the formation of $\text{C}_6\text{H}_3\text{D}_3$ resulting from an exclusive deuterium atom loss channel. Therefore, no atomic hydrogen was emitted from the methyl moiety of the 1-propynyl radical (CH_3CC).

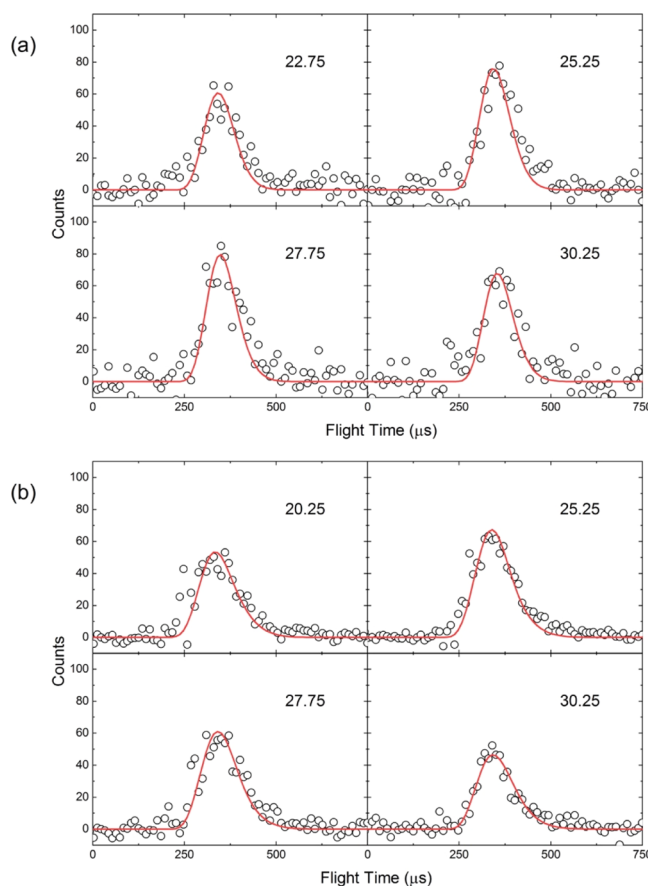
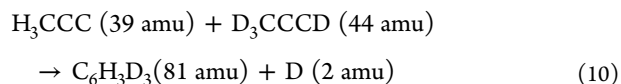
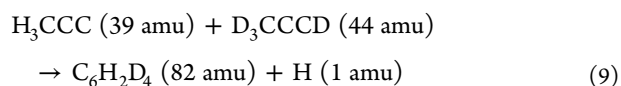
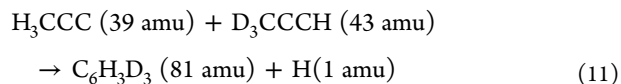


Figure 1. TOF spectra recorded at mass-to-charge (m/z) 78 (C_6H_6^+) from the reaction of 1-propynyl (CH_3CC ; X^2A_1) with (a) methylacetylene (CH_3CCH , X^1A_1) and (b) allene (CH_2CCH_2 ; X^1A_1). The open circles are experimental data, and the red lines are the best fits.



To further pinpoint the position of the deuterium loss from the methylacetylene reactant—methyl or ethynyl group—data were collected in the 1-propynyl (CH_3CC ; 39 amu)–methyl- d_3 -acetylene (CD_3CCH ; 43 amu) system at $m/z = 81$ ($\text{C}_6\text{H}_3\text{D}_3^+$) (11) and $m/z = 80$ ($\text{C}_6\text{H}_4\text{D}_2^+$) (12) for potential hydrogen and/or deuterium atom losses from the acetylenic hydrogen and/or the methyl- d_3 group at methylacetylene. A signal was observed at $m/z = 81$ ($\text{C}_6\text{H}_3\text{D}_3^+$) and $m/z = 80$ ($\text{C}_6\text{H}_4\text{D}_2^+$). Therefore, the signal at $m/z = 81$ suggests the existence of a hydrogen atom replacement (reaction 11); since the aforementioned data reveal that no atomic hydrogen was lost from the methyl group, for the 1-propynyl (CH_3CC)–methyl- d_3 -acetylene (CD_3CCH) system, the hydrogen atom can only be emitted from the ethynyl (CCH) moiety.



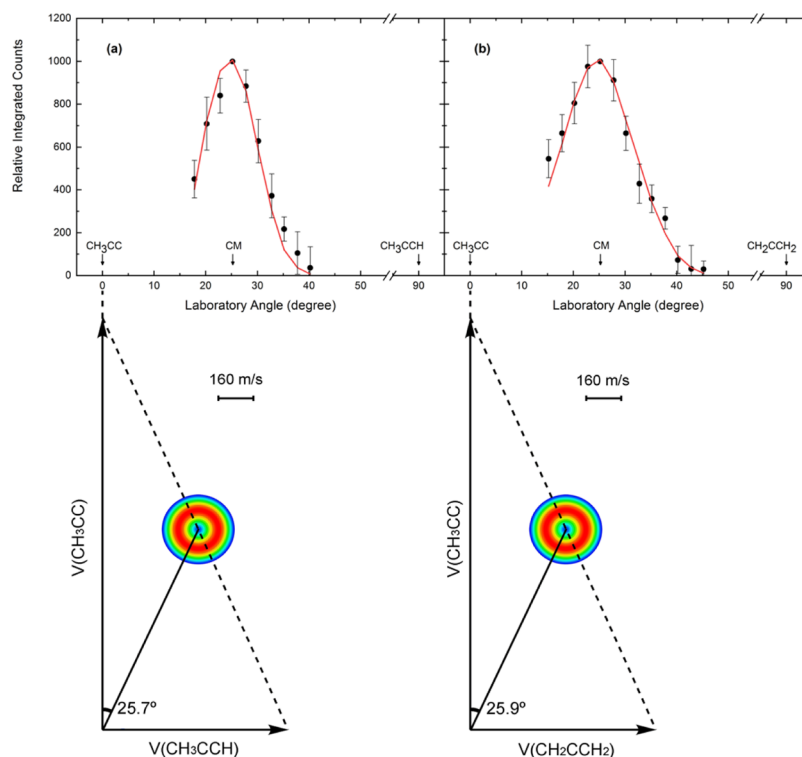
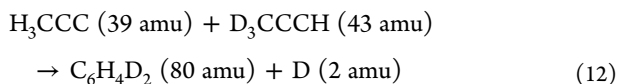
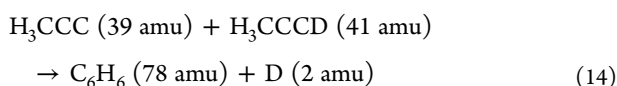
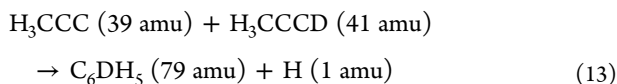


Figure 2. LADs recorded at a mass-to-charge (m/z) ratio of 78 ($C_6H_6^+$) in the reaction of 1-propynyl (CH_3CC ; X^2A_1) with (a) methylacetylene (CH_3CCH , X^1A_1) and (b) allene (CH_2CCH_2 ; X^1A_1). The circles define the experimental data, and the red lines represent the fitting based on the best-fit CM functions depicted in Figure 1. Error bars are $\pm 1\sigma$. The CM arrow indicates the CM angle. The corresponding Newton diagrams relating the LAB reactant and CM frame product velocities are shown below each respective angular distribution. The C_6H_6 product flux is inlaid within the Newton circle (colored), which has a radius equal to the maximum CM velocity of C_6H_6 as defined by the CM functions depicted in Figure 1.

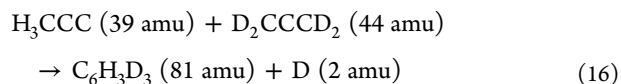
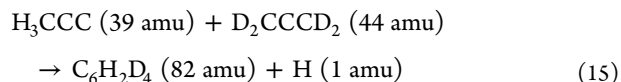


Further, a set of data was collected for the reaction of the 1-propynyl radical (CH_3CC ; 39 amu) with methylacetylene- d_1 (CH_3CCD ; 41 amu) to probe the hydrogen and/or deuterium losses (Figure 3c). Ion counts were observable at $m/z = 79$ ($C_6DH_5^+$) (reaction 13) and $m/z = 78$ ($C_6H_6^+$) (reaction 14). The data at $m/z = 79$ suggest that the hydrogen atom is lost from the methyl group of the methylacetylene reactant. Note that ion counts at $m/z = 78$ can also arise from dissociative electron impact ionization of the product C_6DH_5 formed via reaction 13. Therefore, the results from the 1-propynyl radical (CH_3CC)–methylacetylene- d_1 (CH_3CCD) system demonstrate the existence of a second hydrogen loss channel—besides reaction 9—from the methyl group (reaction 13). Accounting for the ^{13}C isotopic contributions totaling to 6.6% for six carbon atoms and integrating the ion counts, the branching ratio of the hydrogen atom loss from the ethynyl group versus the methyl group of the methylacetylene reactant is determined to be 9.4 ± 0.1 .



Finally, the reaction of the 1-propynyl radical (CH_3CC ; 39 amu) with allene- d_4 (D_2CCCD_2 ; 44 amu) gauged to what

extent the hydrogen loss occurs from the propynyl and/or from the allene reactant. We probed the reactive scattering signals at $m/z = 82$ ($C_6H_2D_4^+$) (reaction 15) and $m/z = 81$ ($C_6H_3D_3^+$) (reaction 16) and observed a strong signal at both the mass-to-charge ratios. This suggests that at least the atomic hydrogen loss is open (reaction 15); once again, the signal at $m/z = 81$ could also arise from dissociative electron impact ionization of the neutral $C_6H_2D_4$ product, so it is difficult to experimentally pin down the contribution of reaction 16. Because of the associated costs of the (partially) deuterated chemicals, data were only collected at the CM angles.



In summary, the isotopic experiments reveal that for the 1-propynyl (CH_3CC)–methylacetylene (CH_3CCH) system, the hydrogen loss originates solely from methylacetylene with branching ratios of the ethynyl versus methyl group of 9.4 ± 0.1 . However, for the reactions of the 1-propynyl radical (CH_3CC) with allene (CH_2CCH_2), the hydrogen loss originates at least from the 1-propynyl radical.

3.2. CM Frame. In both the reactions of the 1-propynyl radical (CH_3CC ; 39 amu) with methylacetylene (CH_3CCH ; 40 amu) and allene (CH_2CCH_2 ; 40 amu), TOFs and LAD angular distribution can be fit using a single reaction channel with the products of the generic formula C_6H_6 and atomic hydrogen. The best-fitting CM functions are shown in

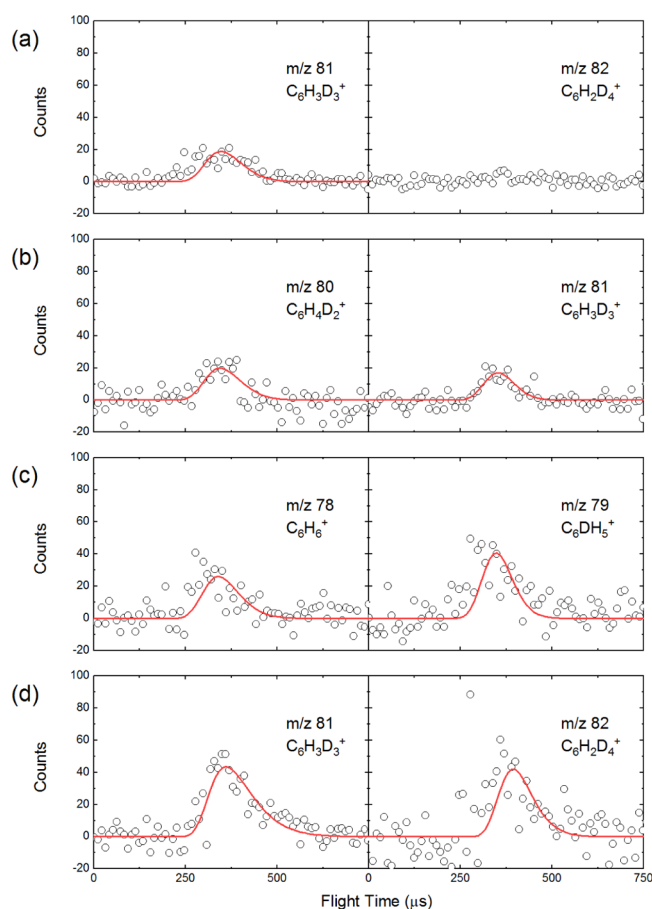


Figure 3. TOF spectra for the reaction of 1-propynyl (CH_3CC ; X^2A_1) with (a) methylacetylene- d_4 (CD_3CCD), (b) methyl- d_3 -acetylene (CD_3CCH), (c) methylacetylene- d_1 (CH_3CCD), and (d) allene- d_4 (CD_2CCD_2) leading to D- and H-loss products. The open circles represent the experimental data, and the red line represents the fit obtained from the forward convolution routine.

Figure 4. The hatched areas of the $P(E_T)$ and $T(\theta)$ functions are determined within the 1σ error limits of the LAB angular distribution along with the peak velocities and speed ratios. It is important to highlight that both the systems reveal striking differences in the reaction energies. The maximum energy E_{max} of each CM translational energy distribution $P(E_T)$ (Figure 4a,b) is represented by the sum of the collision energy and the reaction energy, $E_{\text{max}} = E_C - \Delta_r G$. For the reactive scattering of the 1-propynyl radical (CH_3CC ; 39 amu) with methylacetylene (CH_3CCH ; 40 amu), the maximum $P(E_T)$ was derived to be $159 \pm 19 \text{ kJ mol}^{-1}$ suggesting a reaction energy of $-122 \pm 19 \text{ kJ mol}^{-1}$ to form C_6H_6 along with atomic hydrogen loss. The distribution maximum of $P(E_T)$ at 23 kJ mol^{-1} indicates a tight exit transition state leading to C_6H_6 formation. An average translational energy of $69 \pm 8 \text{ kJ mol}^{-1}$ suggests that only 43% of the energy is channeled into product translation, thus proposing an indirect reaction mechanism. On the other hand, for the reactive scattering experiment of the 1-propynyl radical (CH_3CC ; 39 amu) with allene (CH_2CCH_2 ; 40 amu), the maximum $P(E_T)$ terminates significantly higher at $305 \pm 18 \text{ kJ mol}^{-1}$, deriving a reaction energy of $-269 \pm 18 \text{ kJ mol}^{-1}$ for C_6H_6 along with atomic hydrogen. The distribution maximum of $P(E_T)$ at 59 kJ mol^{-1} suggests that C_6H_6 is formed via a tight exit transition state as well.

Additional information on the reaction dynamics can be obtained by inspecting the CM angular distribution $T(\theta)$. For the reaction of the 1-propynyl radical (CH_3CC ; 39 amu) with methylacetylene (CH_3CCH ; 40 amu), the CM angular distribution $T(\theta)$ (Figure 4a) displays nonzero intensity over all angular range, suggesting that the product was formed via indirect scattering dynamics via activated C_6H_7 complex(es). Second, the forward-backward symmetry of $T(\theta)$ suggests the lifetime of the intermediate being longer than its rotational period. For the reaction of the 1-propynyl radical (CH_3CC) with allene (CH_2CCH_2), the CM angular distribution $T(\theta)$ (Figure 4b) displays similar features compared to the reaction of the 1-propynyl radical (CH_3CC) with methylacetylene (CH_3CCH ; 40 amu). $T(\theta)$, with a nonzero intensity at all angles and forward-backward symmetry, indicates that the product was formed via a relatively long-lived activated C_6H_7 complex via indirect scattering dynamics as well.

4. DISCUSSION

In the case of polyatomic systems such as the reactions of the 1-propynyl radical with methylacetylene (Figures 5–9; Tables 2 and 3) and allene (Figures 10–13; Tables 4 and 5), it is beneficial to combine experimental data with the electronic structure and statistical calculations to elucidate the underlying reaction mechanism(s).

4.1. 1-Propynyl–Methylacetylene System. For the 1-propynyl–methylacetylene system, the electronic structure calculations identified five exit channels (**p1–p5**) leading via indirect scattering dynamics through multiple C_6H_7 intermediates (**i1–i7**) through atomic hydrogen loss (**p1–p3**, **p5**) and methyl radical elimination (**p4**) to distinct C_6H_6 and C_5H_4 isomers (Figure 5). With the exception of **p5** ($+2 \text{ kJ mol}^{-1}$), the reactions are overall exoergic by $276–98 \text{ kJ mol}^{-1}$. A comparison of the computed reaction energies for the atomic hydrogen loss with the experimentally determined reaction energy of $-122 \pm 19 \text{ kJ mol}^{-1}$ suggests the formation of at least the dimethyldiacetylene ($\text{CH}_3\text{CCCCCH}_3$) isomer along with atomic hydrogen (**p1**). On the basis of the reaction energies leading to **p2** and **p5**, these isomers might be masked by the low energy tail of the CM translational energy distribution. How can the dimethyldiacetylene molecule be formed? Our calculations revealed four barrier-less entrance channels dictated by the addition of the 1-propynyl radical (CH_3CC) with its radical center to the carbon–carbon triple bond at C1 and/or C2 of methylacetylene leading to the cis/trans doublet radical intermediates [**i1**]/[**i2**] and [**i3**]/[**i4**], respectively. Considering the destabilizing steric interaction with the methyl group, [**i3**] and [**i4**] are less stable by 14 kJ mol^{-1} compared to [**i1**] and [**i2**]. Each cis/trans isomer pair can be converted by a low barrier of only $18–25 \text{ kJ mol}^{-1}$. The cyclic intermediate [**i5**] interconverts [**i1**] and [**i3**] through the migration of the 1-propynyl group; [**i5**] can lose a hydrogen atom forming the 1-methyltriafulvene isomer (**p5**). Intermediates [**i6**] and [**i7**] are the results of hydrogen migrations in [**i1**] and [**i2**] from the former ethynyl or methyl moieties of the methylacetylene reactant; these hydrogen shifts have significant barriers between 117 and 184 kJ mol^{-1} . Most importantly, intermediates [**i1**] and [**i2**] can undergo unimolecular decomposition via atomic hydrogen loss via tight exit transition states located 24 and $11–12 \text{ kJ mol}^{-1}$ above the energy of the separated products **p1** and **p2**, respectively. Therefore, based on the experimentally derived energetics along with the electronic structure calculations, we can reveal that the

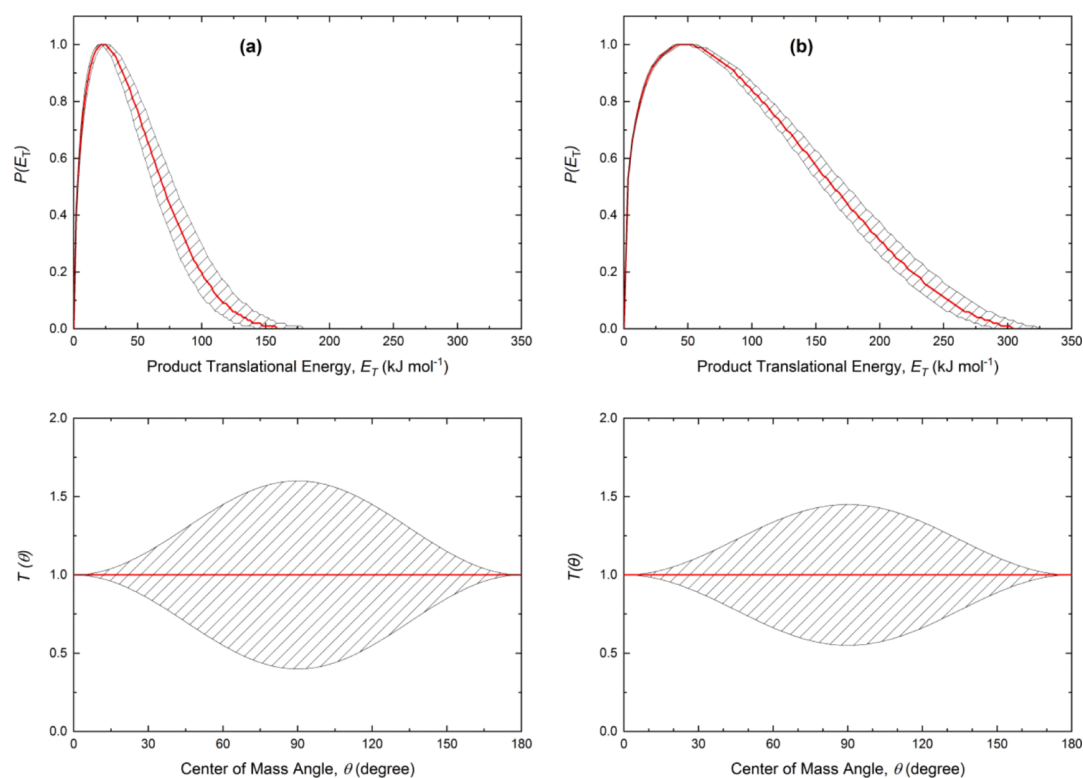


Figure 4. CM functions for the formation of C_6H_6 via atomic hydrogen loss in the reactions of 1-propynyl (CH_3CC ; X^2A_1) with (a) methylacetylene (CH_3CCH , X^1A_1) and (b) allene (CH_2CCH_2 ; X^1A_1). Top: Translational energy flux distributions; bottom: angular flux distributions. The hatched areas define regions of acceptable fits.

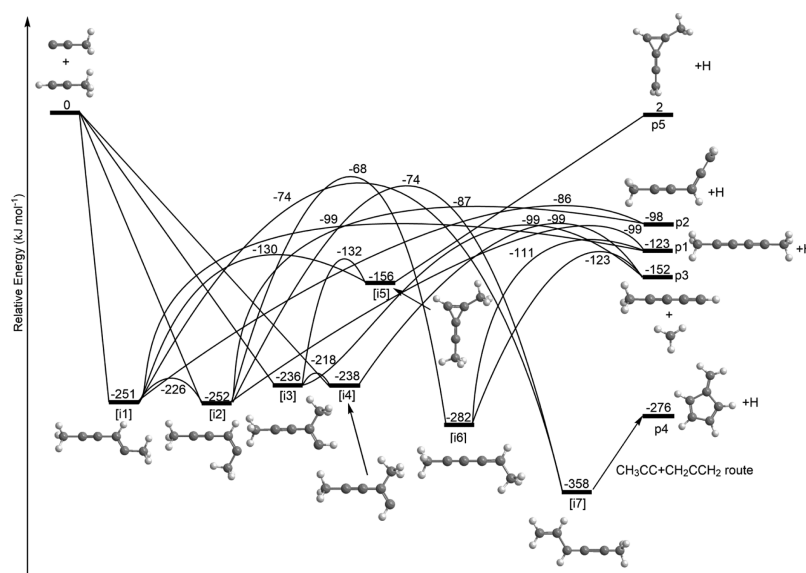


Figure 5. PES for the bimolecular reaction of the 1-propynyl (CH_3CC ; X^2A_1) radical with methylacetylene (CH_3CCH , X^1A_1).

1-ethynyl radical adds with its radical center without entrance barrier to the sterically more accessible C1 atom of methylacetylene forming [i1] and/or [i2], which can interconvert easily. Hereafter, these initial collision complexes can lose a hydrogen atom via tight exit transition state(s) forming at least the dimethyldiacetylene ($CH_3CCCCCH_3$) isomer (p1). The indirect scattering dynamics via long-lived C_6H_7 reaction intermediate(s) and the tight nature of at least one exit transition state are also verified by the CM functions (Section 3.2), with the CM translational energy distribution peaking at around

23 $kJ mol^{-1}$. It should be noted that because of the mismatch of the computed ($-276 kJ mol^{-1}$) and experimentally derived reaction energies ($-122 \pm 19 kJ mol^{-1}$), the fulvene (p4) isomer is not formed. This pathway would require the involvement of the intermediate [i7] along with multiple isomerization processes (Section 4.2).

Having identified the dimethyldiacetylene ($CH_3CCCCCH_3$) isomer (p1) as at least one reaction product, we are attempting to reconcile the results of the isotopic substitution experiments (Section 3.1) with the aforementioned findings that (a) the

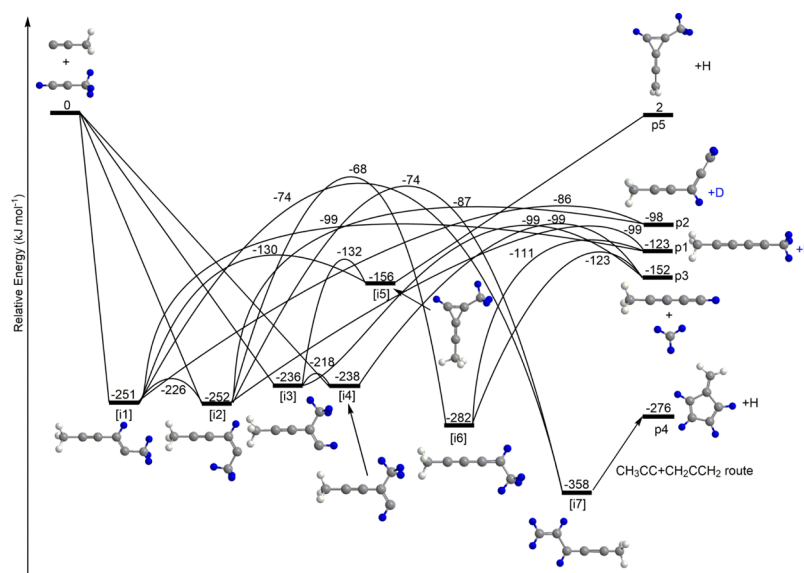


Figure 6. PES for the bimolecular reaction of the 1-propynyl (CH_3CC ; X^2A_1) radical with methylacetylene- d_4 (CD_3CCD ; X^1A_1).

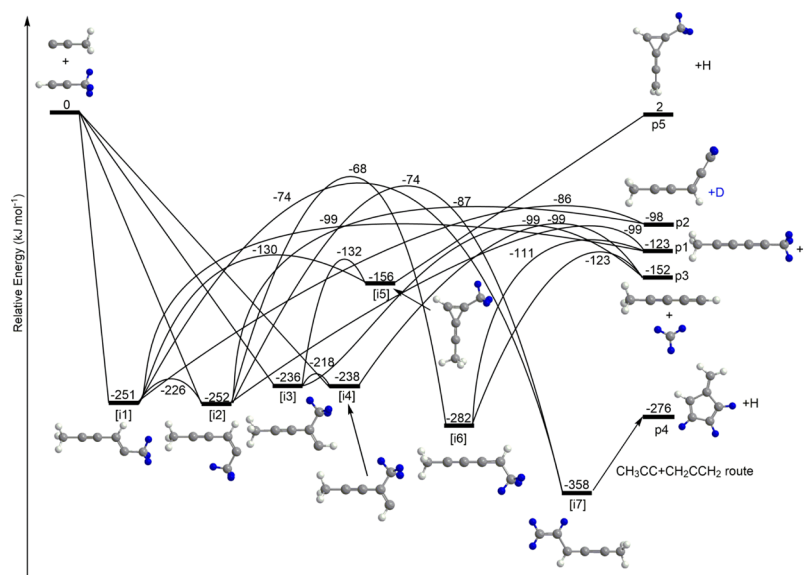


Figure 7. PES for the bimolecular reaction of the 1-propynyl (CH_3CC ; X^2A_1) radical with methyl- d_3 -acetylene (CD_3CCH ; X^1A_1).

hydrogen atom is emitted from the methylacetylene reactant and not from the methyl group of the 1-propynyl reactant and (b) two distinct C_6H_6 isomers are formed via hydrogen atom loss from the ethynyl and methyl groups of the methylacetylene reactant with a branching ratio of 9.4 ± 0.1 . Figures 6–8 trace the position of the deuterium atoms incorporated in the methylacetylene reactants. Most important, the sole detection of the 1-propynyl–methylacetylene- d_4 system provides clear evidence that neither the **p4** nor the **p5** isomer is formed because their pathways are solely connected with the loss of atomic hydrogen but not deuterium (Figure 6). On the other hand, the formation of **p1** and **p2** can fully account for the deuterium loss pathway. With the exclusion of **p4** and **p5**, the 1-propynyl–methylacetylene- d_3 system (Figure 7) provides conclusive evidence that **p1**—dimethyldiacetylene ($\text{CH}_3\text{CCCCCH}_3$)—is formed. Tagging the deuterium atoms reveals that in principle, **p4**, **p1**, and **p5** can account for atomic hydrogen loss; since **p4** and **p5** were already excluded (Figure 6), only **p1** remains as a possible

product of the hydrogen atom loss; this labeling experiment verifies the aforementioned identification of the dimethyldiacetylene isomer. Finally, the 1-propynyl–methylacetylene- d_1 system (Figure 8) helps to identify a second channel. Here, **p2**, **p3**, and **p5** would correlate with an atomic hydrogen loss; however, since **p4** and **p5** were already excluded (Figure 6), only **p2** remains as a possible product of the hydrogen atom loss, revealing that propynylallene ($\text{H}_3\text{CCCHCCCH}$) is formed via decomposition of **[i1]** and/or **[i2]**. These pathways are compiled in Figure 9.

To further test our findings, statistical RRKM calculations were conducted to predict the branching ratios of the products, assuming that a complete energy randomization in the reaction intermediate takes place (Tables 2 and 3). The initial approach discriminates the attack of the 1-propynyl radical at the C1 (Table 2) and C2 carbon atoms of methylacetylene (Table 3). For the atomic hydrogen loss, at our collision energy of 37.1 kJ mol^{-1} , the statistical calculations predict a predominant formation of **p1** and **p2** with a branching ratio of $8.0 \pm 0.2/1.0$;

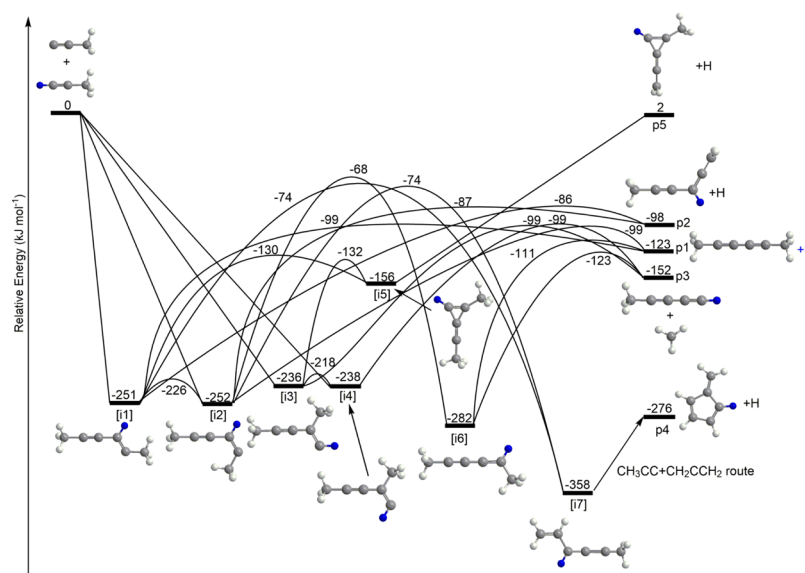


Figure 8. PES for the bimolecular reaction of the 1-propynyl (CH_3CC ; X^2A_1) radical with methylacetylene- d_1 (CH_3CCD ; X^1A_1).

here, the uncertainty in the branching ratios was evaluated by varying the energies of critical transition states by $\pm 4 \text{ kJ mol}^{-1}$ —the expected uncertainty in relative energies. This branching ratio agrees very well with our experimentally determined result of 9.4 ± 0.1 if the 1-propynyl radical only attacks the C1 carbon atom of the methylacetylene reactant. This ratio only slightly varies with the collision energy from 11.1 to 7.7 when the collision energy increases from 0 to 41.8 kJ mol^{-1} . An attack at the C2 carbon atom would also result in a branching ratio of **p1** versus **p2** of $9.0 \pm 0.2/1.0$. However, the methyl loss channel—which was unobserved experimentally with upper limits of 15%—should dominate the scattering dynamics if the 1-propynyl radical adds to the C2 carbon atom. Therefore, the mismatch between the predicted methyl versus atomic hydrogen for the C2 attack and the agreement with the branching ratio for the hydrogen loss and lack of methyl elimination pathway would support an initial addition of the 1-propynyl radical to the C1-atom of methylacetylene—the sterically preferred addition site.

In summary, the reaction dynamics of the 1-propynyl–methylacetylene system are dictated by an initial barrierless addition of the 1-propynyl radical with its radical center to the sterically more accessible C1 carbon atom of the methylacetylene reactant leading via indirect scattering dynamics to intermediate(s) [i1] and/or [i2]. These intermediates are likely to interconvert to each other, considering the low barrier of only 25 kJ mol^{-1} . Upon unimolecular decomposition of these collision complexes via tight exit transition states, both dimethyldiacetylene **p1** ($\text{CH}_3\text{CCCCCH}_3$) and 1-propynylallene **p2** ($\text{H}_2\text{CCCHC-CCH}$) are formed in overall exoergic reactions with an experimental branching ratio of 9.4 ± 0.1 compared to $8.0 \pm 0.2/1.0$, as predicted by RRKM calculations. The formation of these isomers requires the energy to “flow” from the initially formed carbon–carbon single bond over one and three bonds to form the final **p1** and **p2** products, respectively. It shall be noted that the experimental branching ratio was derived based on partially deuterated systems, whereas the RRKM studies exploited fully hydrogenated reactants; this might explain the slight quantitative disagreement.

4.2. 1-Propynyl–Allene System. Considering the 1-propynyl–allene system, the electronic structure calculations

reveal the possible existence of 11 channels (**p1**–**p11**) leading via indirect scattering dynamics through multiple C_6H_7 intermediates (**i1**–**i23**) to atomic hydrogen loss (**p1**–**p5** and **p9**–**p10**) and elimination of heavy fragments [methyl CH_3 (**p6**); vinyl C_2H_3 (**p7**); and acetylene C_2H_2 (**p8** and **p11**)] in overall exoergic reactions (-406 to -12 kJ mol^{-1}) (Figures 10–13, Tables 4 and 5). Once again, a comparison of the computationally predicted reaction energies for the atomic hydrogen loss channel with the experimentally determined reaction energy of $-269 \pm 19 \text{ kJ mol}^{-1}$ correlates well with the formation of at least the formation of the fulvene isomer (**p4**) (-280 kJ mol^{-1}). Fits attempting the inclusion of the thermodynamically more favorable benzene (**p5**) channel yield TOF spectra too fast and a LAD distribution too broad. On the other hand, fits accounting for the formation of 1-propynylallene (**p2**) yield simulated TOFs being too slow and a LAB angular distribution too narrow. However, based on energetical constraints alone, the isomers **p1**–**p3** and **p10** might be hidden within the low-energy section of the CM translational energy distribution. Can the results from the 1-propynyl–allene- d_4 system eliminate any pathways? Recall that at least the atomic hydrogen elimination from the methyl group of the 1-propynyl was observed. This can account for the formation of **p3**, **p4**, **p5**, and **p10** (Figures 11 and 12). Recall that the assumption of a benzene (**p5**) channel cannot fit the experimental data since the fits resulted in TOF spectra being too fast and a LAD distribution too broad. Therefore, the data of the isotopic experiment along with the energetics of the reaction propose that at least fulvene (**p4**) and possibly **p3** and/or **p10** are formed as well with both higher energy isomers masked in the low-energy section of the CM translational energy distribution.

On the basis of our electronic structure calculations, the 1-propynyl radical may add to the terminal or the central carbon atom of allene, forming intermediates [i1]/[i2] and [i3], respectively, without barrier to addition. Considering the barrierless nature of the reaction, large impact parameters should dominate, and hence the 1-propynyl radical should add preferentially to one of the terminal carbon atoms of allene.⁷⁰ This position of addition is also favored by the electrophilic 1-propynyl radical because it preferentially adds to the carbon atom of the allene molecule with the highest electron density (C1/C3: -0.46 ;

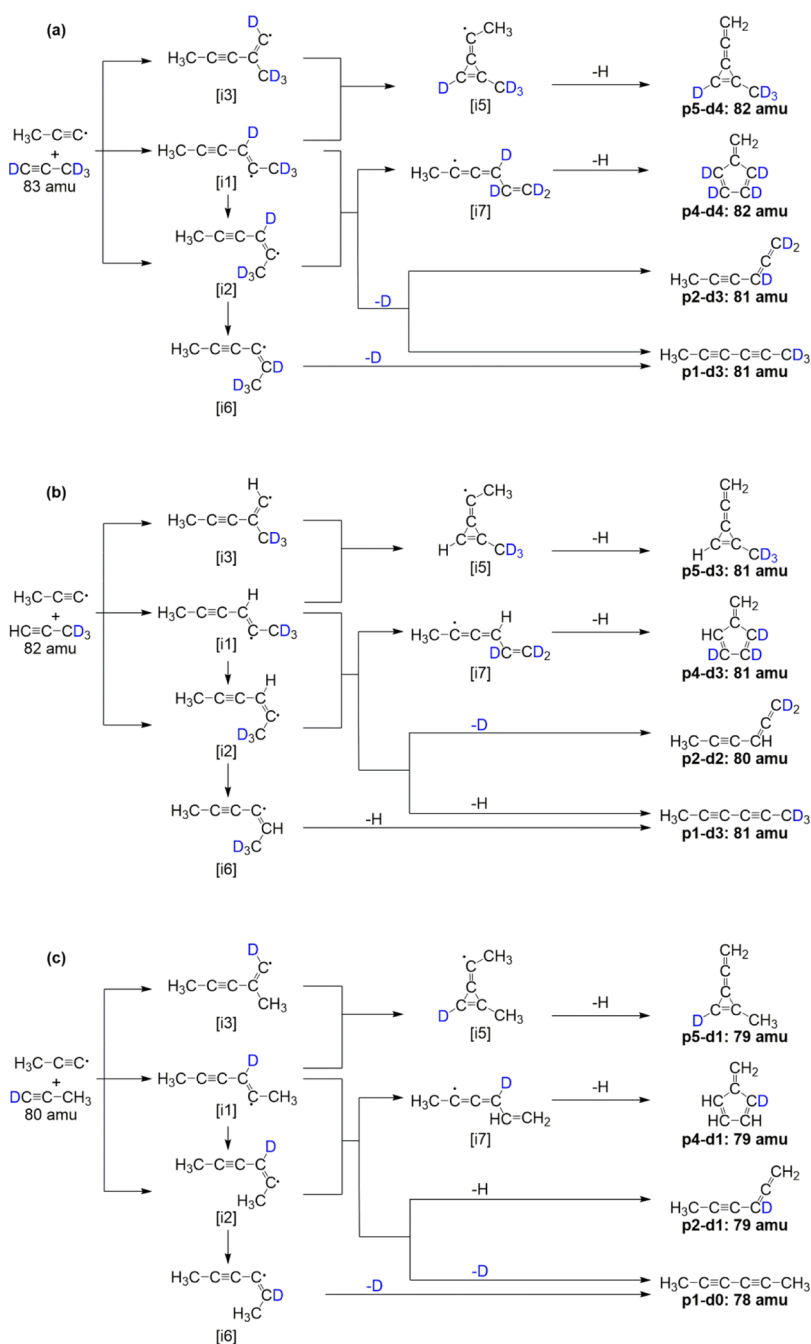


Figure 9. Reaction schematic for the reaction of 1-propynyl (CH_3CC ; X^2A_1) with (a) methylacetylene- d_4 (CD_3CCD), (b) methyl- d_3 -acetylene (CD_3CCH), and (c) methylacetylene- d_1 (CH_3CCD), leading to D- and H-loss products.

Table 2. Statistical Branching Ratios (%) from Intermediate i1 for the Reaction of the 1-Propynyl (CH_3CC) Radical with Methylacetylene (H_3CCCH) at Various Collision Energies^a

	E_c (kJ mol ⁻¹)				
	0	12.6	25.1	37.1	41.8
p1	80.1	81.6	82.5	82.9	82.9
p2	7.2	8.3	9.4	10.3	10.7
p3	12.5	9.8	7.8	6.5	6.1
p4	0.2	0.3	0.3	0.3	0.4
p5	0.0	0.0	0.0	0.0	0.0

^aHere, p1–p5 are dimethyldiacetylene, hexa-1,2-dien-4-yne, methylacetylene, fulvene, and 1-methyl-3-vinylidenecycloprop-1-ene.

Table 3. Statistical Branching Ratios (%) from Intermediate i3 for the Reaction of the 1-Propynyl (CH_3CC) Radical with Methylacetylene (H_3CCCH) at Various Collision Energies^a

	E_c (kJ mol ⁻¹)				
	0	12.6	25.1	37.1	41.8
p1	5.6	4.3	3.3	2.7	2.5
p2	0.5	0.4	0.4	0.3	0.3
p3	93.8	95.3	96.3	96.9	97.2
p4	0.0	0.0	0.0	0.0	0.0
p5	0.0	0.0	0.0	0.0	0.0

^aHere, p1–p5 are dimethyldiacetylene, hexa-1,2-dien-4-yne, methylacetylene, fulvene, and 1-methyl-3-vinylidenecycloprop-1-ene.

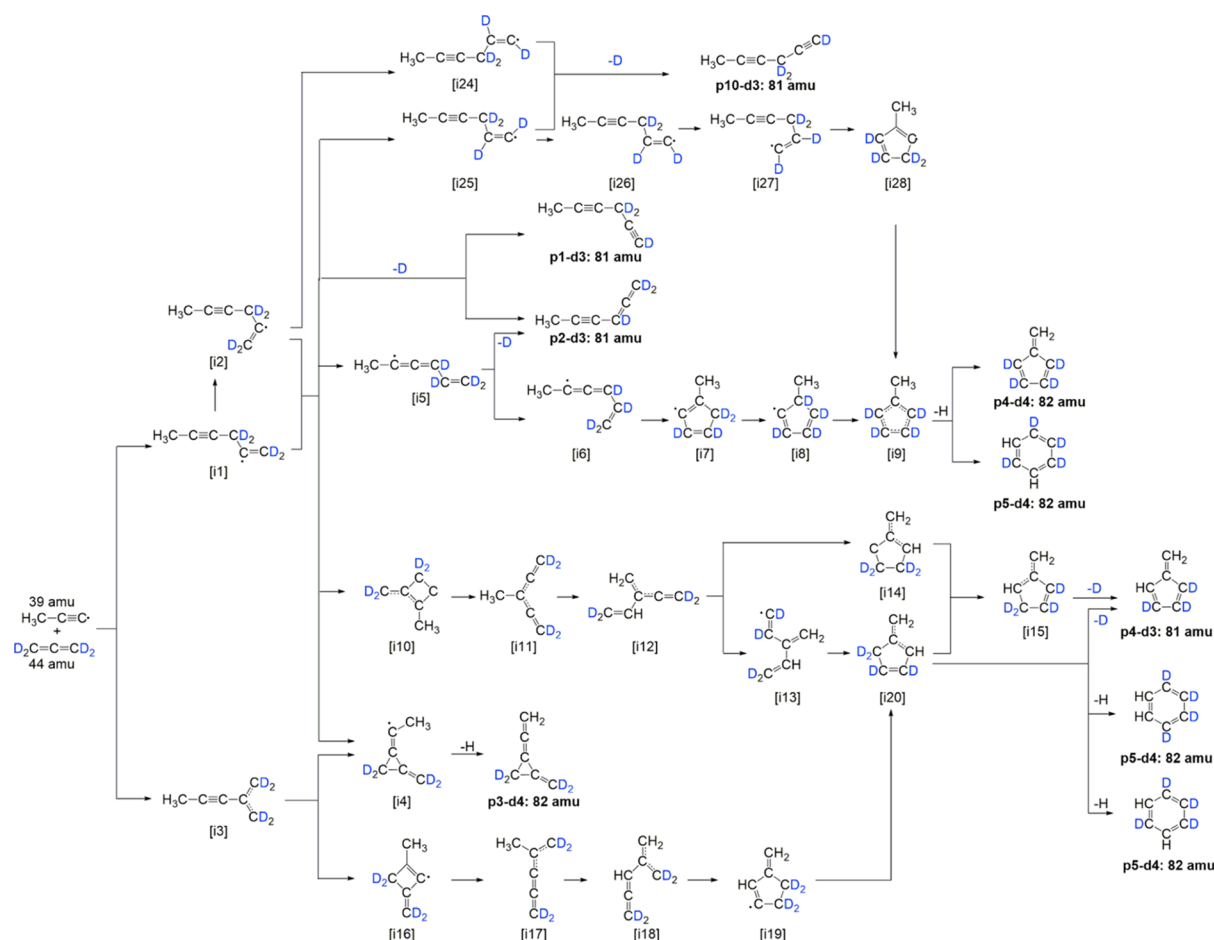


Figure 12. Reaction schematic for the reaction of 1-propynyl (CH_3CC ; X^2A_1) with allene- d_4 (CD_2CCD_2), leading to D- and H-loss products.

C_2 ; +0.08 according to the calculated natural atomic charges).^{65,71} As a matter of fact, reactions of allene with isolobal ethynyl (C_2H)⁷¹ and cyano (CN)⁶⁵ radicals studied under single collision conditions in our laboratory revealed that the doublet radical reactant solely added to the terminal C1/C3 carbon atoms of allene. Therefore, we might expect an (almost) exclusive addition of the 1-propynyl radical to the terminal C1/C3 atoms of allene leading to [i1]/[i2]. It should be noted though that the addition of the 1-propynyl radical to the C2 carbon would produce a resonantly stabilized radical [i3], which is 105 kJ mol^{-1} lower in energy than [i1]/[i2]. The intermediates [i3] and [i1]/[i2] can interconvert relatively easily via barriers, which are lower than those for any of their decomposition channels. With respect to the formation of fulvene, we are focusing now on the 1-propynyl–allene- d_4 system and the experimentally verified atomic hydrogen loss (Figures 11 and 12). Note that two distinct fulvene isotopologues can be formed via atomic hydrogen (from [i9]) and deuterium loss (from [i15] and [i20]). The reaction pathways leading solely to fulvene- d_4 are compiled in Figure 12. Here, two key reaction pathways can be identified. From the initial adduct [i1], the “low barrier” six-step reaction sequence [i1] \rightarrow [i5] \rightarrow [i6] \rightarrow [i7] \rightarrow [i8] \rightarrow [i9] \rightarrow fulvene + hydrogen involves three hydrogen shifts, cis–trans isomerization, and cyclization with inherent barriers ranging lower than 70 kJ mol^{-1} with respect to the separated reactants. Note that [i1] can also isomerize to [i2] prior to a hydrogen shift leading to [i5]. A second “high barrier” eight-step pathway involves the sequence [i1] \rightarrow [i2] \rightarrow [i24] \rightarrow [i25] \rightarrow [i26] \rightarrow [i27] \rightarrow [i28] \rightarrow fulvene + hydrogen with a

Table 4. Statistical Branching Ratios (%) from Intermediate i1/i2 for the Reaction of the 1-Propynyl (CH_3CC) Radical with Allene (H_2CCCH_2) at Various Collision Energies^a

	E_C (kJ mol^{-1})				
	0	12.6	25.1	36.5	41.8
p1	54.9	63.5	69.5	73.3	74.7
p2	16.4	16.2	15.6	15.0	14.7
p3	0.0	0.0	0.0	0.0	0.0
p4	5.6	4.5	3.8	3.4	3.2
p5	0.4	0.4	0.4	0.3	0.3
p6	0.0	0.0	0.0	0.0	0.0
p7	0.2	0.2	0.2	0.2	0.2
p8	0.0	0.0	0.0	0.0	0.0
p9	22.5	15.0	10.2	7.4	6.5
p10	0.0	0.0	0.0	0.0	0.0
p11	0.1	0.2	0.3	0.4	0.4

^aHere, p1–p11 are hexa-1,4-diyne, penta-1,2-dien-4-yne, 1-methyl-ene-2-vinylidenecyclopropane, fulvene, benzene, cyclopenta-1,2,4-triene, buta-1,2,3-triene, 1,3-butadien-2-yl + acetylene, penta-1,2,3,4-tetraene, hexa-1,4-diyne, and buta-1,2-diene + acetylene.

rate-limiting transition state [i2] \rightarrow [i24] located 36 kJ mol^{-1} below with respect to the separated reactants; note that [i1] can also isomerize to [i25] in one step. Overall, all reaction sequences involve an initial addition of the 1-propynyl radical to the C1/C3 carbon atoms of allene leading to [i1] and eventually form the decomposing intermediate [i9] (Figure 13). On the basis of the energies of the transition states, the

Table 5. Statistical Branching Ratios (%) from Intermediate i3 for the Reaction of the 1-Propynyl (CH_3CC) Radical with Allene (H_2CCCH_2) at Various Collision Energies^a

	E_c (kJ mol ⁻¹)				
	0	12.6	25.1	36.5	41.8
p1	57.2	64.5	69.4	72.5	73.6
p2	20.3	19.6	18.6	17.6	17.2
p3	0.0	0.0	0.0	0.0	0.0
p4	4.2	3.4	2.8	2.5	2.3
p5	0.3	0.3	0.3	0.2	0.2
p6	0.0	0.0	0.0	0.0	0.0
p7	0.2	0.2	0.2	0.2	0.1
p8	0.0	0.0	0.0	0.0	0.0
p9	17.7	12.0	8.7	6.8	6.2
p10	0.0	0.0	0.0	0.0	0.0
p11	0.1	0.1	0.2	0.2	0.3

^aHere, p1–p11 are hexa-1,4-diyne, penta-1,2-dien-4-yne, 1-methylene-2-vinylidenecyclopropane, fulvene, benzene, cyclopenta-1,2,4-triene, buta-1,2,3-triene, 1,3-butadien-2-yl + acetylene, penta-1,2,3,4-tetraene, hexa-1,4-diyne, and buta-1,2-diene + acetylene.

“low barrier route” to fulvene should be preferred among various fulvene formation pathways. However, statistical RRKM calculations (Tables 4 and 5) only propose a relatively small branching ratio of fulvene (2.5–3.4%) with isomers p1 and p2 suggested to dominate. We should recall that our aforementioned discussions could not rule out the formation of

thermodynamically less stable isomers; further, isomers p1 and p2 should be formed exclusively via atomic deuterium loss (Figure 11), which was masked in the 1-propynyl–allene- d_4 system because of dissociative ionization of the $\text{C}_6\text{H}_2\text{D}_4$ parent (Section 3.2). Therefore, fulvene can be clearly identified as a reaction product, albeit with small branching ratios, with predicted scattering signal arising for p1 and p2. Note that the failed identification absence of benzene formation can be rationalized through a comparison of the barriers involved in the benzene versus fulvene formation (Figure 10). The formation of benzene (p5) has to proceed via the sequence [i9] → [i21] → [i22] → [i23] → benzene + hydrogen where the computed rate constant for the rate limiting isomerization, [i9] → [i21], is $2.3 \times 10^8 \text{ s}^{-1}$. The computed rate constant for the competing decomposition of the [i9] isomer to fulvene + H bimolecular product is higher by a factor of 6, $1.4 \times 10^9 \text{ s}^{-1}$.

5. SUMMARY

Crossed molecular beam reactions of the 1-propynyl radical (CH_3CC ; X^2A_1) with two C_3H_4 isomers, methylacetylene (H_3CCCH ; X^1A_1) and allene (H_2CCCH_2 ; X^1A_1), along with their (partially) deuterated counterparts were investigated at collision energies of around 37 kJ mol^{-1} to elucidate the chemical reaction dynamics to form distinct C_6H_6 isomers under single collision conditions. The forward convolution fitting of the LADs and TOF spectra combined with ab initio and statistical (RRKM) calculations exposed that both systems have no entrance barrier, proceed via indirect (complex-forming)

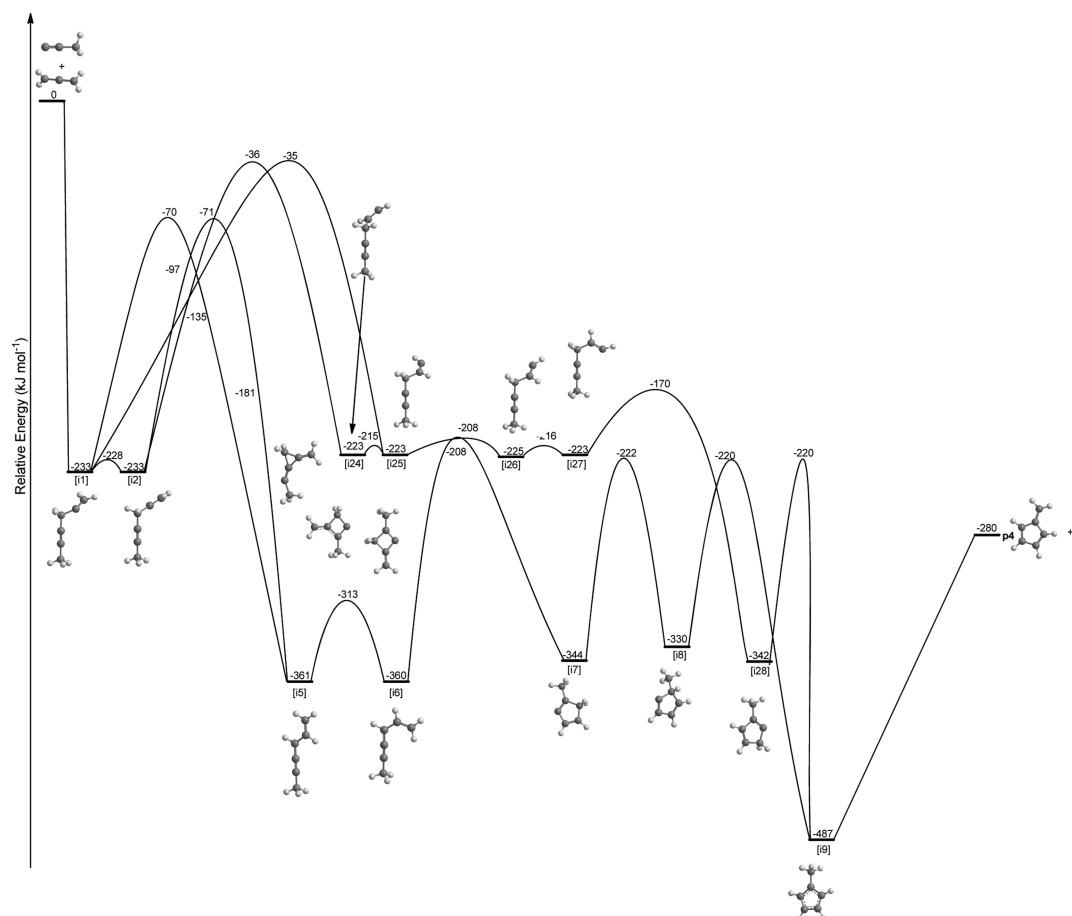


Figure 13. Reduced PES for the reaction of 1-propynyl (CH_3CC ; X^2A_1) with allene (CH_2CCH_2) leading to fulvene. The pathways have been extracted based on the detection of the hydrogen atom loss pathway in the 1-propynyl–allene- d_4 system.

reaction dynamics involving C_6H_7 , holding life times longer than their rotation period(s), and are initiated by the addition of the 1-propynyl radical with its radical center to the π -electron density of the unsaturated hydrocarbon at the terminal carbon atoms of methylacetylene (C1) and allene (C1/C3). In the methylacetylene system, the experimental data and computations can be reconciled by proposing that the initial collision complex [i1] and possibly [i2], which can easily interconvert to [i1], undergo unimolecular decomposition via tight exit transition states through atomic hydrogen loss, yielding dimethyldiacetylene **p1** ($CH_3CCCCCH_3$) and 1-propynylallene **p2** ($H_2CCCHCCCH$) in overall exoergic reactions (123 and 98 kJ mol^{-1}) with an experimental branching ratio of 9.4 ± 0.1 . In simple terms, the formation of these isomers requires the energy to “flow” from the initially formed carbon–carbon single bond over one and three bonds to form the products **p1** and **p2**, respectively, suggesting that the methyl group of the 1-propynyl reactant acts solely as a spectator. Here, the pathway to fulvene, [i1] \rightarrow [i7] \rightarrow **p4**, requires hydrogen atom migration from the methyl group in the methylacetylene moiety via a 177 kJ mol^{-1} barrier. For comparison, the atomic hydrogen elimination pathways to the **p1** and **p2** products exhibit 152 and 165 kJ mol^{-1} barriers, respectively, and also are favored by entropy. The computed rate constant for the [i1] \rightarrow [i7] isomerization, 9.6×10^6 s^{-1} , is much lower than those for the hydrogen atom elimination pathways [i1] \rightarrow **p1**, 2.3×10^9 s^{-1} and [i1] \rightarrow **p2**, 2.9×10^8 s^{-1} . As a result, the reaction dynamics of the 1-propynyl–methylacetylene system mirror the reaction mechanisms unraveled for the ethynyl (C_2H)–methylacetylene^{66,72} and cyano (CN)–methylacetylene^{63,65,73} systems studied previously. These reactions are also initiated by the barrierless addition of the doublet radical reactant with its radical center at the carbon atom to the sterically more accessible C1 carbon atom holding the acetylenic hydrogen atom; for each system, the reaction intermediates decompose via two exit channels via tight exit transition states, leading to cyanomethylacetylene (CH_3CCCN) [1] along with cyanoallene ($H_2CCCHCN$) [4] and methylacetylene (CH_3CCCH) [2] together with ethynylallene ($H_2CCCHCCH$) [3], with cyanomethylacetylene and methylacetylene being lower in energy by typically 17 kJ mol^{-1} compared to their allene-type isomers (Figure 14). On the other hand, in the allene system, our experimental investigations propose the formation of the fulvene ($c-C_5H_4CH_2$) isomer via a six-step reaction sequence with two higher energy isomers—hexa-1,2-dien-4-yne ($H_2CCCHCCCH_3$) and hexa-1,4-diyne ($HCCCH_2CCCH_3$)—predicted based on our statistical calculations. While the pathways to these acyclic C_6H_6 isomers are statistically preferable, peculiar vibrational features of the initial complexes [i1]/[i2] may favor the fulvene formation channel dynamically. In particular, these complexes possess two low-energy vibrational modes of about 71 and 140 cm^{-1} , which include significant contributions of CCC and CCH bending involving the central CH_2 group and thus could promote the hydrogen atom shift from CH_2 to the neighboring carbon atom, that is, the [i1]/[i2] \rightarrow [i5] rearrangement, and then starting from [i5], the channel to produce fulvene overwhelmingly dominates statistically. High-energy content in these low-frequency bending modes from the initial chemical activation may increase the life time of [i1]/[i2] and hence make the rearrangement to [i5] and eventual yield to fulvene more likely than predicted by the statistical calculations. This hypothesis on the non-RRKM behavior may be tested in the

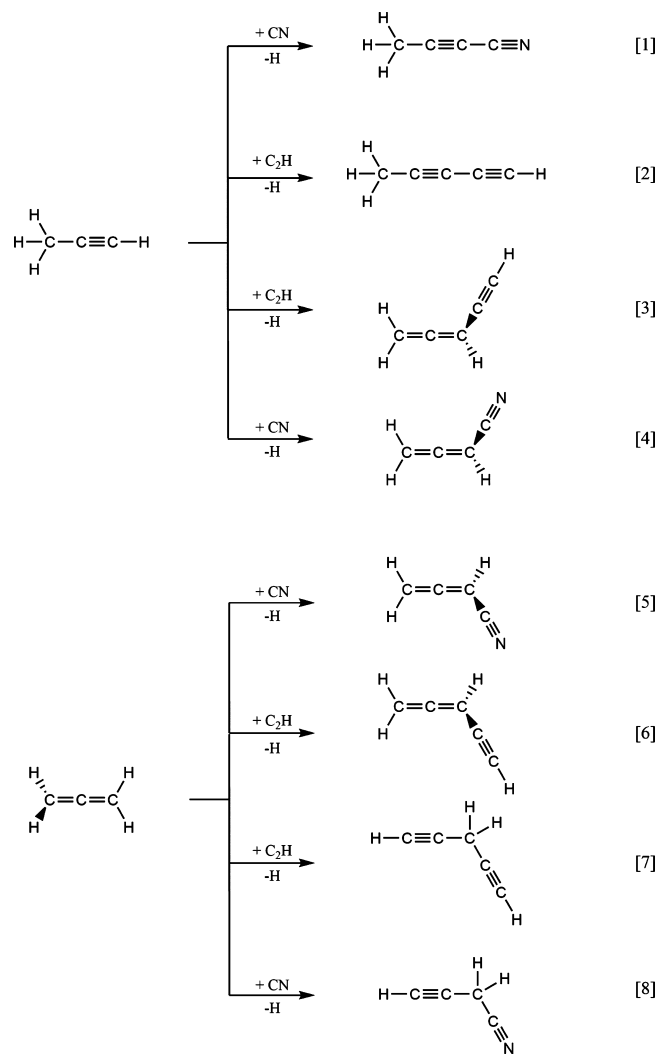


Figure 14. Product channels detected in the reaction of methylacetylene and allene with ethynyl (C_2H) and cyano (CN) radicals under single collision conditions.

future via quasi-classical trajectory calculations, that is, a direct dynamics study on flight, which at present remains a very challenging and extremely computationally demanding task. The pathway to fulvene is quite unique compared to the reactions of allene with the isolobal ethynyl (C_2H) and cyano radicals (CN) (Figure 14) and advocates that in the allene–1-propynyl system, the methyl group of the 1-propynyl reactant is actively engaged in the reaction mechanism to form fulvene. Finally, it is important highlighting that since both reactions are barrierless and exoergic and all transition states reside below the energy of the separated reactants, all hydrogen-deficient C_6H_6 isomers inferred in our investigation are predicted to be synthesized in low-temperature environments such as in hydrocarbon rich atmospheres of planets and their moons such as Titan, holding mole fractions up to a few 10^{-5} at 900 km,^{74,75} along with cold molecular clouds such as Taurus Molecular Cloud-1. Considering the isolobal concept of the ethynyl and the 1-propynyl radicals, the reactions of 1-propynyl with both methylacetylene and allene are expected to proceed with rate constants of a few 10^{-10} cm^3s^{-1} similar to those rates determined for the ethynyl–allene and ethynyl–methylacetylene systems.⁷⁶ Here, the 1-propynyl radical can be generated via photodissociation of methylacetylene⁷⁷ both in our solar

system and in the ISM; upon reaction with methylacetylene and/or allene, the hitherto undetected C_6H_6 isomers, hexa-1,2-dien-4-yne ($H_2CCCHCCCH_3$) (0.45 D), hexa-1,4-diyne (H_3CCCCH_2CCH) (0.80 D), methylacetylene (CH_3CCCCH) (1.28 D), and fulvene ($c-C_5H_4CH_2$) (0.23 D), can be searched for in deep space by exploiting the Atacama Large Millimeter/submillimeter Array.

■ ASSOCIATED CONTENT

● Supporting Information

The Supporting Information is available free of charge on the ACS Publications website at DOI: 10.1021/acs.jpca.9b03746.

Optimized cartesian coordinates and vibrational frequencies for all intermediates, transition states, reactants, and products involved in the reactions of the propynyl radical with C_3H_4 isomers, methylacetylene and allene (PDF)

■ AUTHOR INFORMATION

Corresponding Authors

*E-mail: mebela@fui.edu (A.M.M.).

*E-mail: ralfk@hawaii.edu (R.I.K.).

ORCID

Aaron M. Thomas: 0000-0001-8540-9523

Alexander M. Mebel: 0000-0002-7233-3133

Ralf I. Kaiser: 0000-0002-7233-7206

Notes

The authors declare no competing financial interest.

■ ACKNOWLEDGMENTS

This work was supported by the U.S. Department of Energy, Basic Energy Sciences by grants DE-FG02-03ER15411 and DE-FG02-04ER15570 to the University of Hawaii and to the Florida International University, respectively.

■ REFERENCES

- (1) Jones, B. M.; Zhang, F.; Kaiser, R. I.; Jamal, A.; Mebel, A. M.; Cordiner, M. A.; Charnley, S. B. Formation of Benzene in the Interstellar Medium. *Proc. Nat. Acad. Sci. U.S.A.* **2011**, *108*, 452–457.
- (2) Alzueta, M. U.; Glarborg, P.; Dam-Johansen, K. Experimental and Kinetic Modeling Study of the Oxidation of Benzene. *Int. J. Chem. Kinet.* **2000**, *32*, 498–522.
- (3) Richter, H.; Howard, J. B. Formation and consumption of single-ring aromatic hydrocarbons and their precursors in premixed acetylene, ethylene and benzene flames. *Phys. Chem. Chem. Phys.* **2002**, *4*, 2038–2055.
- (4) Miller, J. A.; Klippenstein, S. J.; Georgievskii, Y.; Harding, L. B.; Allen, W. D.; Simmonett, A. C. Reactions between Resonance-Stabilized Radicals: Propargyl + Allyl†. *J. Phys. Chem. A* **2010**, *114*, 4881–4890.
- (5) Senosiain, J. P.; Miller, J. A. The Reaction of *n*- and *i*- C_4H_5 Radicals with Acetylene. *J. Phys. Chem. A* **2007**, *111*, 3740–3747.
- (6) McEnally, C. S.; Pfefferle, L. D.; Atakan, B.; Kohse-Höinghaus, K. Studies of Aromatic Hydrocarbon Formation Mechanisms in Flames: Progress towards Closing the Fuel Gap. *Prog. Energy Combust. Sci.* **2006**, *32*, 247–294.
- (7) Jasper, A. W.; Hansen, N. Hydrogen-Assisted Isomerizations of Fulvene to Benzene and of Larger Cyclic Aromatic Hydrocarbons. *Proc. Combust. Inst.* **2013**, *34*, 279–287.
- (8) Cernicharo, J.; Heras, A. M.; Pardo, J. R.; Tielens, A. G. G. M.; Guélin, M.; Dartois, E.; Neri, R.; Waters, L. B. F. M. Infrared Space Observatory's Discovery of C_4H_2 , C_6H_2 , and Benzene in CRL 618. *Astrophys. J.* **2001**, *546*, L127.
- (9) Tielens, A. G. G. M. Interstellar Polycyclic Aromatic Hydrocarbon Molecules. *Annu. Rev. Astron. Astr.* **2008**, *46*, 289–337.
- (10) Miller, J. A.; Klippenstein, S. J. The Recombination of Propargyl Radicals and Other Reactions on a C_6H_6 Potential. *J. Phys. Chem. A* **2003**, *107*, 7783–7799.
- (11) Westmoreland, P. R.; Dean, A. M.; Howard, J. B.; Longwell, J. P. Forming Benzene in Flames by Chemically Activated Isomerization. *J. Phys. Chem.* **1989**, *93*, 8171–8180.
- (12) Lindstedt, R. P.; Skevis, G. Detailed Kinetic Modeling of Premixed Benzene Flames. *Combust. Flame* **1994**, *99*, 551–561.
- (13) Zhang, H.-Y.; McKinnon, J. T. Elementary Reaction Modeling of High-Temperature Benzene Combustion. *Combust. Sci. Technol.* **1995**, *107*, 261–300.
- (14) Moskaleva, L. V.; Mebel, A. M.; Lin, M. C. The $CH_3 + C_5H_5$ Reaction: A Potential Source of Benzene at High Temperatures. *Symposium (International) on Combustion*; Elsevier, 1996; Vol. 26, pp 521–526.
- (15) Dinadayalane, T. C.; Priyakumar, U. D.; Sastry, G. N. aExploration of C_6H_6 Potential Energy Surface: A Computational Effort to Unravel the Relative Stabilities and Synthetic Feasibility of New Benzene Isomers†. *J. Phys. Chem. A* **2004**, *108*, 11433–11448.
- (16) Sivaramakrishnan, R.; Brezinsky, K.; Vasudevan, H.; Tranter, R. S. A Shock-Tube Study of the High-Pressure Thermal Decomposition of Benzene. *Combust. Sci. Technol.* **2006**, *178*, 285–305.
- (17) Kislov, V. V.; Mebel, A. M. Ab Initio G3-type/Statistical Theory Study of the Formation of Indene in Combustion Flames. I. Pathways Involving Benzene and Phenyl Radical†. *J. Phys. Chem. A* **2007**, *111*, 3922–3931.
- (18) Giguere, P. T.; Clark, F. O.; Snyder, L. E.; Buhl, D.; Johnson, D. R.; Lovas, F. J. Upper Limits for Interstellar Fulvene and Nitric Acid. *Astrophys. J.* **1973**, *182*, 477–479.
- (19) Ruiterkamp, R.; Peeters, Z.; Moore, M. H.; Hudson, R. L.; Ehrenfreund, P. A Quantitative Study of Proton Irradiation and UV Photolysis of Benzene in Interstellar Environments. *Astron. Astrophys.* **2005**, *440*, 391–402.
- (20) Shimoyama, A.; Naraoka, H.; Komiya, M.; Harada, K. Analyses of Carboxylic Acids and Hydrocarbons in Antarctic Carbonaceous Chondrites, Yamato-74662 and Yamato-793321. *Geochem. J.* **1989**, *23*, 181–193.
- (21) Coustenis, A.; Salama, A.; Schulz, B.; Ott, S.; Lellouch, E.; Encrenaz, T. h.; Gautier, D.; Feuchtgruber, H. Titan's atmosphere from ISO mid-infrared spectroscopy. *Icarus* **2003**, *161*, 383–403.
- (22) Nagendrappa, G. Benzene and its Isomers. *Resonance* **2001**, *6*, 74–78.
- (23) Madden, L. K.; Mebel, A. M.; Lin, M. C.; Melius, C. F. Theoretical study of the thermal isomerization of fulvene to benzene. *J. Phys. Org. Chem.* **1996**, *9*, 801–810.
- (24) Mebel, A. M.; Lin, S. H.; Yang, X. M.; Lee, Y. T. Theoretical Study on the Mechanism of the Dissociation of Benzene. The $C_5H_3 + CH_3$ Product Channel. *J. Phys. Chem. A* **1997**, *101*, 6781–6789.
- (25) Mebel, A. M.; Lin, M. C.; Chakraborty, D.; Park, J.; Lin, S. H.; Lee, Y. T. Ab initio Molecular Orbital/Rice–Ramsperger–Kassel–Marcus Theory Study of Multichannel Rate Constants for the Unimolecular Decomposition of Benzene and the $H + C_6H_5$ Reaction over the Ground Electronic State. *J. Chem. Phys.* **2001**, *114*, 8421–8435.
- (26) Mebel, A. M. Dissociation, Isomerization, and Isotope Scrambling of Benzene: A Theoretical View. *Reviews of Modern Quantum Chemistry: A Celebration of the Contributions of Robert G Parr (In 2 Volumes)*; World Scientific, 2002; pp 340–358.
- (27) Kislov, V. V.; Nguyen, T. L.; Mebel, A. M.; Lin, S. H.; Smith, S. C. Photodissociation of benzene under collision-free conditions: An ab initio/Rice–Ramsperger–Kassel–Marcus study. *J. Chem. Phys.* **2004**, *120*, 7008–7017.
- (28) Thiele, J. Ueber Ketonreactionen bei dem Cyclopentadien. *Chem. Ber.* **1900**, *33*, 666–673.
- (29) Alkemade, U.; Homann, K. H. Formation of C_6H_6 Isomers by Recombination of Propynyl in the System Sodium Vapor Propynylhalide. *Z. Phys. Chem. Neue. Fol.* **1989**, *161*, 19–34.

- (30) Thomas, S.; Communal, F.; Westmoreland, P. C_3H_3 Reaction Kinetics in Fuel-rich Combustion. *Prep. Fuel Chem. ACS* **1991**, *36*, 1448.
- (31) Tranter, R. S.; Tang, W.; Anderson, K. B.; Brezinsky, K. Shock Tube Study of Thermal Rearrangement of 1,5-Hexadiyne over Wide Temperature and Pressure Regime. *J. Phys. Chem. A* **2004**, *108*, 3406–3415.
- (32) <http://www.astrochymist.org>. (accessed April 20, 2019).
- (33) Bezdard, B.; Drossart, P.; Encrenaz, T.; Feuchtgruber, H. Benzene on the Giant Planets. *Icarus* **2001**, *154*, 492–500.
- (34) Kim, S.; Caldwell, J.; Rivolo, A.; Wagener, R.; Orton, G. S. Infrared polar brightening on Jupiter III. Spectrometry from the Voyager 1 IRIS experiment. *Icarus* **1985**, *64*, 233–248.
- (35) Tranter, R. S.; Yang, X.; Kiefer, J. H. Dissociation of C_3H_3I and Rates for C_3H_3 Combination at High Temperatures. *Proc. Combust. Inst.* **2011**, *33*, 259–265.
- (36) Balucani, N.; Mebel, A. M.; Lee, Y. T.; Kaiser, R. I. A Combined Crossed Molecular Beam and ab Initio Study of the Reactions $C_2(X^1\Sigma_g^+, a^3\Pi_u) + C_2H_4 \rightarrow n-C_4H_3(X^2A')$ and $H(^2S_{1/2})$. *J. Phys. Chem. A* **2001**, *105*, 9813–9818.
- (37) Krasnoukhov, V. S.; Porfiriev, D. P.; Zavershinskiy, I. P.; Azyazov, V. N.; Mebel, A. M. Kinetics of the $CH_3 + C_3H_3$ Reaction: A Theoretical Study. *J. Phys. Chem. A* **2017**, *121*, 9191–9200.
- (38) Zhang, F.; Jones, B.; Maksyutenko, P.; Kaiser, R. I.; Chin, C.; Kislov, V. V.; Mebel, A. M. Formation of the Phenyl Radical [$C_6H_5(X^2A_1)$] under Single Collision Conditions: a Crossed-Molecular Beam and ab Initio Study. *J. Am. Chem. Soc.* **2010**, *132*, 2672–2683.
- (39) Sharma, S.; Green, W. H. Computed Rate Coefficients and Product Yields for $c-C_3H_5 + CH_3 \rightarrow$ Products. *J. Phys. Chem. A* **2009**, *113*, 8871–8882.
- (40) Hansen, N.; Miller, J. A.; Taatjes, C. A.; Wang, J.; Cool, T. A.; Law, M. E.; Westmoreland, P. R. Photoionization Mass Spectrometric Studies and Modeling of Fuel-Rich Allene and Propyne Flames. *Proc. Combust. Inst.* **2007**, *31*, 1157–1164.
- (41) Hansen, N.; Miller, J. A.; Westmoreland, P. R.; Kasper, T.; Kohse-Höinghaus, K.; Wang, J.; Cool, T. A. Isomer-Specific Combustion Chemistry in Allene and Propyne Flames. *Combust. Flame* **2009**, *156*, 2153–2164.
- (42) Gazi, A.; Vourliotakis, G.; Skevis, G.; Founti, M. A Modelling Study of Allene and Propyne Combustion in Flames. *Proceedings of Fifth European Combustion Meeting ECM2011*, Cardiff, U.K., 2011.
- (43) Kaiser, R. I.; Maksyutenko, P.; Ennis, C.; Zhang, F.; Gu, X.; Krishtal, S. P.; Mebel, A. M.; Kostko, O.; Ahmed, M. Untangling the chemical evolution of Titan's atmosphere and surface-from homogeneous to heterogeneous chemistry. *Faraday Discuss.* **2010**, *147*, 429–478.
- (44) Thomas, A. M.; Zhao, L.; He, C.; Mebel, A. M.; Kaiser, R. I. A Combined Experimental and Computational Study on the Reaction Dynamics of the 1-Propynyl (CH_3CC)-Acetylene ($HCCH$) System and the Formation of Methylidyne (CH_3CCCCH). *J. Phys. Chem. A* **2018**, *122*, 6663–6672.
- (45) Brink, G. O. Electron Bombardment Molecular Beam Detector. *Rev. Sci. Instrum.* **1966**, *37*, 857–860.
- (46) Daly, N. R. Scintillation Type Mass Spectrometer Ion Detector. *Rev. Sci. Instrum.* **1960**, *31*, 264–267.
- (47) Vernon, M. F. Molecular Beam Scattering. Ph. D. Dissertation, University of California, Berkeley, CA, 1983.
- (48) Weiss, P. S. The Reaction Dynamics of Electronically Excited Alkali Atoms with Simple Molecules. Ph.D. Dissertation, University of California, Berkeley, CA, 1986.
- (49) Kaiser, R. I.; Hahndorf, I.; Huang, L. C. L.; Lee, Y. T.; Bettinger, H. F.; Schleyer, P. v. R.; Schaefer, H. F., III; Schreiner, P. R. Crossed Beams Reaction of Atomic Carbon, $C(^3P_j)$, with D_6 -Benzene, $C_6D_6(X^1A_{1g})$: Observation of the Per-deutero-1, 2-Didehydro-Cycloheptatrienyl Radical, $C_7D_5(X^2B_2)$. *J. Chem. Phys.* **1999**, *110*, 6091–6094.
- (50) Kaiser, R. I.; Mebel, A. M.; Chang, A. H. H.; Lin, S. H.; Lee, Y. T. Crossed-Beam Reaction of Carbon Atoms with Hydrocarbon Molecules. V. Chemical Dynamics of $n-C_4H_3$ Formation from Reaction of $C(^3P_j)$ with Allene, $H_2CCCH_2(X^1A_1)$. *J. Chem. Phys.* **1999**, *110*, 10330–10344.
- (51) Becke, A. D. Density-functional thermochemistry. III. The role of exact exchange. *J. Chem. Phys.* **1993**, *98*, 5648–5652.
- (52) Lee, C.; Yang, W.; Parr, R. G. Development of the Colle-Salvetti Correlation-Energy Formula into a Functional of the Electron Density. *Phys. Rev. B: Condens. Matter* **1988**, *37*, 785.
- (53) Adler, T. B.; Knizia, G.; Werner, H.-J. A Simple and Efficient CCSD(T)-F12 Approximation. *J. Chem. Phys.* **2007**, *127*, 221106.
- (54) Knizia, G.; Adler, T. B.; Werner, H.-J. Simplified CCSD(T)-F12 methods: Theory and benchmarks. *J. Chem. Phys.* **2009**, *130*, 054104.
- (55) Dunning, T. H., Jr Gaussian Basis Sets for Use in Correlated Molecular Calculations. I. The Atoms Boron through Neon and Hydrogen. *J. Chem. Phys.* **1989**, *90*, 1007–1023.
- (56) Zhang, J.; Valeev, E. F. Prediction of Reaction Barriers and Thermochemical Properties with Explicitly Correlated Coupled-Cluster Methods: a Basis Set Assessment. *J. Chem. Theory Comput.* **2012**, *8*, 3175–3186.
- (57) Frisch, M. J.; Trucks, G.; Schlegel, H. B.; Scuseria, G.; Robb, M.; Cheeseman, J.; Scalmani, G.; Barone, V.; Mennucci, B.; Petersson, G. *Gaussian 09*, revision A. 1; Gaussian Inc.: Wallingford CT, 2009; Vol. 27, p 34.
- (58) Werner, H.; Knowles, P.; Knizia, G.; Manby, F.; Schütz, M.; Celani, P.; Korona, T.; Lindh, R.; Mitrushenkov, A.; Rauhut, G. *MOLPRO*, version 2010.1, a Package of ab Initio Programs, 2010, see <http://www.molpro.net>, 2015.
- (59) Holbrook, K. A.; Pilling, M. J.; Robertson, S. H. *Unimolecular Reactions*; Wiley, 1996.
- (60) Eyring, H.; Lin, S.; Lin, S. *Basic Chemical Kinetics*; John Wiley & Sons, Inc.: New York, NY, 1983.
- (61) Steinfeld, J. I.; Francisco, J. S.; Hase, W. L. *Chemical Kinetics and Dynamics*; Prentice Hall: Englewood Cliffs, New Jersey, 1989; Vol. 3.
- (62) Fernández-Ramos, A.; Miller, J. A.; Klippenstein, S. J.; Truhlar, D. G. Modeling the Kinetics of Bimolecular Reactions. *Chem. Rev.* **2006**, *106*, 4518–4584.
- (63) Huang, L. C. L.; Balucani, N.; Lee, Y. T.; Kaiser, R. I.; Osamura, Y. Crossed Beam Reaction of the Cyano Radical, $CN(X^2\Sigma^+)$, with Methylacetylene, $CH_3CCH(X^1A_1)$: Observation of Cyanopropyne, $CH_3CCC(CN)(X^1A_1)$, and Cyanoallene, $H_2CCCHCN(X^1A')$. *J. Chem. Phys.* **1999**, *111*, 2857–2860.
- (64) Kaiser, R. I.; Stranges, D.; Lee, Y. T.; Suits, A. G. Neutral-Neutral Reactions in the Interstellar Medium. I. Formation of Carbon Hydride Radicals via Reaction of Carbon Atoms with Unsaturated Hydrocarbons. *Astrophys. J.* **1997**, *477*, 982.
- (65) Balucani, N.; Asvany, O.; Kaiser, R.-I.; Osamura, Y. Formation of Three C_4H_3N Isomers from the Reaction of $CN(X^2\Sigma^+)$ with Allene, $H_2CCCH_2(X^1A_1)$, and Methylacetylene, $CH_3CCH(X^1A_1)$: A Combined Crossed Beam and Ab Initio Study. *J. Phys. Chem. A* **2002**, *106*, 4301–4311.
- (66) Stahl, F.; von Ragué Schleyer, P.; Bettinger, H. F.; Kaiser, R. I.; Lee, Y. T.; Schaefer, H. F., III Reaction of the Ethynyl Radical, C_2H , with Methylacetylene, CH_3CCH , under Single Collision Conditions: Implications for Astrochemistry. *J. Chem. Phys.* **2001**, *114*, 3476–3487.
- (67) Kaiser, R. I.; Chiong, C. C.; Asvany, O.; Lee, Y. T.; Stahl, F.; von R. Schleyer, P.; Schaefer, H. F., III Chemical Dynamics of D1-Methylidyne ($CH_3CCC(D)$; X^1A_1) and D1-Ethynylallene ($H_2CCCH(C_2D)$; X^1A') Formation from Reaction of $C_2D(X^2\Sigma^+)$ with Methylacetylene, $CH_3CCH(X^1A_1)$. *J. Chem. Phys.* **2001**, *114*, 3488–3496.
- (68) Balucani, N.; Asvany, O.; Chang, A. H. H.; Lin, S. H.; Lee, Y. T.; Kaiser, R. I.; Bettinger, H. F.; Schleyer, P. v. R.; Schaefer, H. F., III Crossed Beam Reaction of Cyano radicals with hydrocarbon Molecules. II. Chemical Dynamics of 1-cyano-1-methylallene ($CNCH_3CCCH_2$; X^1A') Formation from Reaction of $CN(X^2\Sigma^+)$ with Dimethylacetylene $CH_3CCCH_3(X^1A_1)$. *J. Chem. Phys.* **1999**, *111*, 7472–7479.

(69) Gu, X.; Kaiser, R. I. Reaction Dynamics of Phenyl Radicals in Extreme Environments: a Crossed Molecular Beam Study. *Acc. Chem. Res.* **2008**, *42*, 290–302.

(70) Balucani, N.; Asvany, O.; Huang, L. C. L.; Lee, Y. T.; Kaiser, R. I.; Osamura, Y.; Bettinger, H. F. Formation of Nitriles in the Interstellar Medium via Reactions of Cyano Radicals, $\text{CN}(X^2\Sigma^+)$, with Unsaturated Hydrocarbons. *Astrophys. J.* **2000**, *545*, 892.

(71) Zhang, F.; Kim, S.; Kaiser, R. I. A Crossed Molecular Beams Study of the Reaction of the Ethynyl Radical ($\text{C}_2\text{H}(X^2\Sigma^+)$) with Allene (H_2CCCH_2 (X^1A_1)). *Phys. Chem. Chem. Phys.* **2009**, *11*, 4707–4714.

(72) Kaiser, R. I.; Chiong, C. C.; Asvany, O.; Lee, Y. T.; Stahl, F.; Schleyer, P. v. R.; Schaefer, H. F., III Chemical Dynamics of D1-Methyldiacetylene (CH_3CCCCD ; X^1A_1) and D1-Ethynylallene (H_2CCCH (C_2D); X^1A') Formation from Reaction of $\text{C}_2\text{D}(X^2\Sigma^+)$ with Methylacetylene, CH_3CCH (X^1A_1). *J. Chem. Phys.* **2001**, *114*, 3488–3496.

(73) Chin, Y. N.; Kaiser, R. I.; Lemme, C.; Henkel, C. Detection of Interstellar Cyanoallene and its Implications for Astrochemistry. *AIP Conference Proceedings*; AIP, 2006; pp 149–153.

(74) Kaiser, R. I.; Mebel, A. M. On the Formation of Polyacetylenes and Cyanopolyacetylenes in Titan's Atmosphere and their Role in Astrobiology. *Chem. Soc. Rev.* **2012**, *41*, 5490–5501.

(75) Vuitton, V.; Yelle, R. V.; Klippenstein, S. J.; Hörst, S. M.; Lavvas, P. Simulating the Density of Organic Species in the Atmosphere of Titan with a Coupled Ion-Neutral Photochemical Model. *Icarus* **2019**, *324*, 120–197.

(76) Carty, D.; Le Page, V.; Sims, I. R.; Smith, I. W. M. Low Temperature Rate Coefficients for the Reactions of CN and C_2H Radicals with Allene ($\text{CH}_2=\text{C}=\text{CH}_2$) and Methylacetylene (CH_3CCH). *Chem. Phys. Lett.* **2001**, *344*, 310–316.

(77) Zhou, J.; Garand, E.; Eisfeld, W.; Neumark, D. M. Slow Electron Velocity-Map Imaging Spectroscopy of the 1-Propynyl Radical. *J. Chem. Phys.* **2007**, *127*, 034304.